JOURNAL OF GEOPHYSICAL RESEARCH, VOL. 106, NO. C9, PAGES 19,527–19,546, SEPTEMBER 15, 2001

Velocity structure and transport of the Indonesian Throughflow in the major straits restricting flow into the Indian Ocean

Susan L. Hautala,[1] Janet Sprintall,[2] James T. Potemra,[1] Jackson C. Chong,[2] Wahyu Pandoe,[3] Nan Bray,[4] and A. Gani Ilahude[5]

Abstract. An array of shallow pressure gauge pairs is used to determine shallow geostrophic flow relative to an unknown mean velocity in the five principal straits that separate the eastern Indian Ocean from the interior Indonesian seas (Lombok Strait, Sumba Strait, Ombai Strait, Savu/Dao Straits, and Timor Passage). Repeat transects across the straits over several tidal cycles with a 150-kHz acoustic Doppler current profiler were made during three separate years, and provide a first look at the lateral and vertical structure of the upper throughflow in these straits as well as a means of "leveling" the pressure gauge data to determine the mean shallow velocity and provide transport estimates. We estimate a total 2-year average transport for 1996–1997 through Lombok, Ombai, and Timor Straits as 8.4 ± 3.4 Sv toward the Indian Ocean. The flow structure in the upper 200 m is seen to be similar in Lombok, Sumba, and Ombai Straits, with a division into two layers, governed by different dynamics, where the upper layer episodically flows away from the Indian Ocean. Laterally, flow tends to be strongest in the deepest parts of the channel, with the exception of Lombok Strait which shows a consistent intensification of flow toward the western side. Eastward flowing northern boundary currents in Sumba and Ombai Straits suggest that the South Java Current may penetrate to the Banda Sea, farther eastward than previously documented. Although additional observations are required for a conclusive comparison, the estimated transport time series suggest differences in timing of outflow into the Indian Ocean relative to inflow from the Pacific of a size that could significantly impact the Banda Sea thermocline structure.

1. Introduction

The Indonesian Throughflow is a key element of global circulation, heat, and freshwater balances and is thought to play a critical role in several aspects of the midlatitude general circulation in the Indian and Pacific Oceans as well as Australasian regional climate. A simple scaling argument suggests that a mean through flow of 10 Sv, with mass returned to the Pacific at a temperature appropriate for the pathway south of Australia, produces a heat flux (i.e., thermal energy transport) of ~0.5 PW from the Pacific to the Indian Ocean [*Godfrey*, 1996], a number comparable in magnitude to the total net flux across 24°N in the Pacific [*Bryden et al*., 1991; *MacDonald*, 1998], and roughly one third of the heat transport south through the southern Indian Ocean [*Ganachaud et al*., 2000]. In recent years, a number of programs have measured aspects of the Indonesian Throughflow, revealing an unanticipated richness of spatial and temporal variability. Undoubtedly, playing a principal role is the region's complex geography, with multiple constrictions controlling flow into and out of the Banda Sea, a set of large, deep (3500–7500 m) interconnected basins that receive water from Pacific sources and release to the Indian Ocean water that has been substantially modified in its essential water mass properties [*Rochford*, 1966; *Ffield and Gordon*, 1992; *Hautala et al*., 1996].

Pacific, Indian, and local forcing modulates the through flow on a wide range of timescales which combine to produce variability of the same order as the long-term mean. The Pacific-to-Indian pressure gradient, often cited as the driving force for the throughflow, varies with the seasonal cycle in wind stress. Transport is expected to be maximal during May to September, when flow from the Banda Sea into the Indian Ocean is enhanced by the local Ekman response to the southeast monsoon [*Wyrtki*, 1987]. On semiannual timescales, sea level along the eastern boundary of the Indian Ocean is modulated by Kelvin waves originating in the equatorial Indian Ocean [*Clarke and Liu*, 1993; *Arief and Murray*, 1996; *Sprintall et al*., 1999, 2000]. Intraseasonal variability (30–60 days), forced locally and remotely, is remarkably strong in both observations [*Arief*, 1992; *Molcard et al*., 1994; *Chong et al*., 2000] and models [*Qiu*, 1998; J. T. Potemra et al., Interactions between the Indonesian seas and the Indian Ocean in observations and numerical models, submitted to *Journal of Physical Oceanography*, 2001, hereinafter referred to as Potemra et al., submitted manuscript, 2001]. The observed semiannual variation can be viewed as a twice-annual enhancement of the amplitude of intraseasonal westerly wind events in the Indian Ocean equatorial wind field during the monsoon transition periods (April and November).

[1]School of Oceanography, University of Washington, Seattle, Washington, USA.
[2]Physical Oceanography Research Division, Scripps Institution of Oceanography, University of California, San Diego, La Jolla, California, USA.
[3]Department of Oceanography, Texas A&M University, College Station, Texas, USA.
[4]CSIRO Marine Research, Hobart, Tasmania, Australia.
[5]Indonesian Institute of Sciences, Jakarta, Indonesia.

Paper number 2000JC000577.
0148-0227/01/2000JC000577$09.00

On interannual timescales, conceptual models [*Clarke and Liu*, 1994], numerical results [*Potemra et al*., 1997], and recent observations [*Meyers*, 1996; *Gordon et al*., 1999] all conclude weakened through flow transport during El Niño events in response to lowering of western Pacific sea level. The interannual, El Niño–Southern Oscillation (ENSO)-related, signal is stronger in the eastern part of the archipelago in observations [*Bray et al*., 1996] and numerical models [*Potemra et al*., 1997, submitted manuscript, 2001] consistent with the suggestion of *Clarke and Liu* [1994] that low-frequency energy from the Pacific dominates forcing of the Northwest Australian Shelf.

While some programs focus their measurement efforts on flow from the Pacific Ocean into the Banda Sea [e.g., *Gordon et al*., 1999; *Kashino et al*., 1996], our study examines flow from this key reservoir into the Indian Ocean. The existing data suggest large differences in peak upper ocean transport timing between the "inflow" and "outflow" straits. In this paper, we describe two instrumentation efforts, an array of shallow pressure gauges and a series of repeat ADCP transects across the major outflow straits into the Indian Ocean, which are combined to yield time series of absolute geostrophic surface flow and estimates of upper layer transport. A brief overview of the experiment and preliminary results has been presented by *Chong et al*. [2000]. The role of this paper is to expand upon that synopsis, highlighting the contribution of the acoustic Doppler current profiler (ADCP) data to our understanding of flow structure and total transport. The dynamics responsible for the observed sea level variability and the vertical structure of transport are explored more thoroughly by Potemra et al. (submitted manuscript, 2001).

2. Data Collection and Processing

2.1. Pressure Gauge Data

The eastern edge of the shallow (<75 m) Sunda Shelf, connecting the southeast tip of Kalimantan and the northeast tip of Java, marks the western boundary of the principal through flow route between the Pacific and Indian Oceans passing through a series of deep (>1000 m) basins connected by shallower sills. The Shallow Pressure Gauge Array (SPGA) consists of pressure gauge pairs across the five major outflow straits through the Lesser Sunda Islands between Bali and the Northwest Australian Shelf that are the principal conduits for flow from the interior Indonesian seas to the eastern Indian Ocean (Figure 1). A total of nine pressure gauges were deployed by divers at a depth of 5–10 m. The eight instruments in Indonesian waters were initially deployed in December 1995, redeployed in March 1997 and March 1998, and finally recovered in May 1999. Cross-strait pressure gradient records end prematurely (March 1998) for Savu/Dao Straits because of the disappearance of the South Sumba gauge. The Ombai Strait record is similarly truncated because the regional political situation prevented recovery of the instrument off East Timor. We hope to eventually recover the latter pressure gauge and extend that time series. The pressure gauge at Ashmore reef on the Northwest Australian Shelf was deployed initially in April 1995. It failed early in its second deployment (November 1996), leaving a 9-month gap in the Timor Passage cross-strait pressure gradient record until it was redeployed in August 1997. The Ashmore reef gauge was recovered in October 1998.

Pressure was measured every 3 min by a Paroscientific quartz sensor with an accuracy of 0.3 mbar. The largest error comes from instrument drift, resulting in an apparent decrease in pressure by an estimated 0.3 mbar every year [*Wearn and Larson*, 1982]. The records have not been corrected for drift; however, the error is relatively small compared to the dynamic signal. For example, in Lombok Strait the observed pressure variation is of order 10 mbar. To calculate the low-frequency geostrophic flow, the raw pressure data are first averaged into hourly bins. Tides are removed by fitting 15 tidal frequencies (monthly, fortnightly, diurnal, and semidiurnal) in a least squares sense. Anchor shifts (including the 9-month gap at Ashmore) are dealt with by comparing each record with tides predicted by the harmonic analysis. The time series are then low-pass-filtered to remove signals with period shorter than 5 days. Time series of relative geostrophic flow are computed from the low-pass pressure differences, with the mean removed.

The question naturally arises: Why do we expect the low-frequency along-strait flow to be primarily geostrophic? First, for barotropic steady state conditions, as long as variations in the along-strait direction occur slowly (which is to be expected at some distance from the sill itself), scale analysis shows that the along-strait flow will be largely in geostrophic balance [e.g., *Pratt and Lundberg*, 1991]. *Toulany and Garrett* [1984] examined the time-dependent problem and the extent to which changing sea level differences between two basins induces an along-strait velocity response commensurate with geostrophic Kelvin wave adjustment. Their arguments apply to a strait width less than the Rossby radius of deformation; in the region of the Indonesian outflow straits, the baroclinic Rossby radius is ~70 km (buoyancy frequency $N = 0.014\ \mathrm{s}^{-1}$, vertical depth scale $H = 100$ m). Of the five straits measured by the pressure gauges, only Savu Strait (~90 km wide) and Timor Passage (~100 km wide) are marginally larger that the Rossby radius. Hence applying Toulany and Garrett's solutions, with parameters appropriate to Lombok Strait (width ~37 km; depth ~300 m), suggests that geostrophy holds for $\omega \leq f/3$, corresponding to periods longer than ~10 days, and that variability on intraseasonal to interannual scales will be geostrophic. By comparing midchannel current meter and across-strait pressure difference data in the Strait of Juan de Fuca (comparable in width to the baroclinic Rossby radius), *Labrecque et al*. [1994] found 20-m subtidal velocity (10–20 cm s^{-1} magnitude) at periods longer than 4 days to be highly geostrophic. Similarly, in the SPGA data the geostrophic flow record computed from the pressure difference timeseries in Ombai Strait compares favorably with direct velocity data from a contemporaneous current meter at 25 m [*Chong et al*., 2000]. Finally, Potemra et al. (submitted manuscript, 2001) use a 2.5-layer reduced gravity model to determine a relationship between sea level at each side and upper layer (~250 m) transport through the outflow straits. In each case, the optimal fit occurred when sea level on each side was weighted by nearly equal amounts of opposite sign, confirming the basic geostrophic relationship between upper layer velocity and sea level difference across the straits in the model. They found similar relationships strongly supporting geostrophy in output from the Parallel Ocean Climate Model (POCM) [*Semtner and Chervin*, 1992] for the 0–100 m transport in Ombai Strait and 0–260 m transport in Timor Passage (Lombok Strait is not resolved by the POCM).

We did not directly compute the wind-driven ageostrophic contribution to flow because preliminary calculations suggest that it is small relative to the through flow velocities that are found in the outflow straits. Local wind in the straits is affected by the high orography of the volcanic islands but is weakly

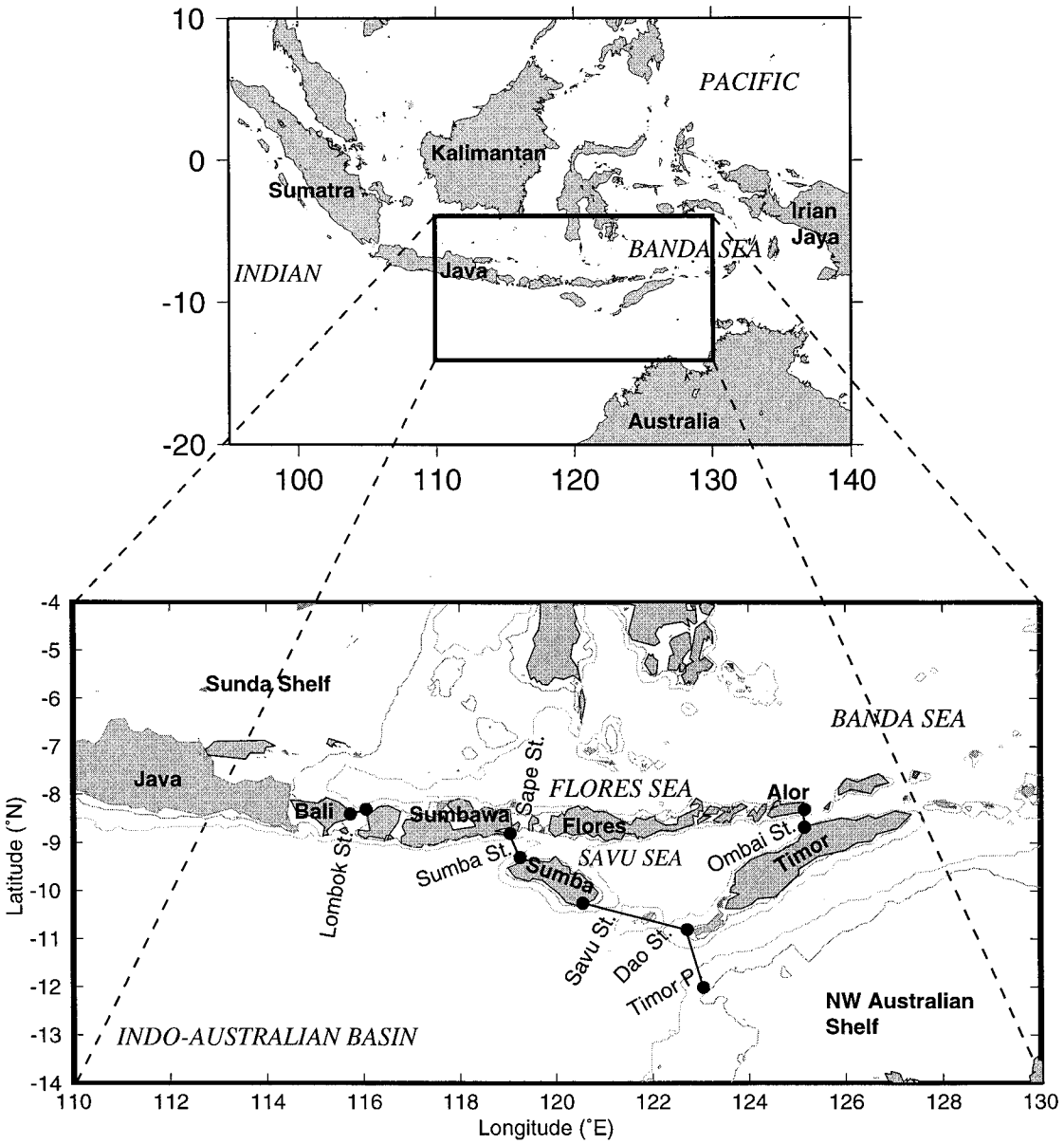

Figure 1. Map showing the locations of the nine instruments that compose the Shallow Pressure Gauge Array (SPGA) spanning the five principal conduits for flow from the interior Indonesian seas to the Indian Ocean. The 200-m and 1000-m isobaths are shown.

correlated ($r = 0.56$) with offshore winds [*Arief*, 1992]. Wind velocities, however, are observed to be much lower in the straits. For example, local wind speeds at meteorological stations on either side of Lombok Strait are typically <6 m s^{-1}, even during intense intraseasonal wind bursts [*Arief*, 1992]. The resulting peak Ekman transport contribution is only $\sim$0.1 Sv, with a layer-average velocity contribution (assuming an Ekman layer at least 25 m thick) of no more than 10 cm s^{-1}, within the typical error of our subtidal velocity estimates. In contrast, the average subtidal velocity in our shallowest ADCP bin at 20–30 m in Lombok Strait is 60–80 cm s^{-1}. Wind stress offshore, as represented, for example, by the European Centre for Medium-Range Weather Forecasts fields, can be an order of magnitude stronger during individual events and may contribute significantly to estimates of flow through sections across the Indo-Australian Basin. In addition, Ekman transport may provide a more significant contribution to the total flow through the combined Savu/Dao Strait, which is relatively wide ($\sim$244 km) and appears to have small subtidal velocities, although our resolution of the tidal cycle at these straits is poor. An accurate characterization of the total flow through Savu/Dao Straits awaits both better local wind and tidal velocity information.

2.2. Collection and Processing of ADCP Data

Acoustic Doppler current profiler (ADCP) data were collected routinely during the deployment, turnaround, and recovery cruises. In addition, repeat transects were made across the five main outflow straits for the purposes of determining the time-average velocity and transport. In 1995, aboard the R/V *Baruna Jaya I*, a towed 150-kHz RD Instruments Broad Band ADCP was used. Subsequent surveys, aboard the R/V

Table 1. Coefficients of Towed ADCP Compass Correction Function

Coefficient	Value, deg
a	-3.46 ± 0.13
b	-0.33 ± 0.19
c	-1.68 ± 0.15
d	0.65 ± 0.18
e	-0.37 ± 0.14

Baruna Jaya IV, made use of a similar vessel-mounted instrument.

For most surveys, single-ping data were recorded in Earth coordinates. Postcruise, the data were reaveraged into 5-min ensembles, rejecting data with an error velocity >20 cm s^{-1}. Average ship speed and direction were computed from Global Positioning Satellite (GPS) data by differencing 30-s averages at the beginning and end of each ensemble. Statistics were also recorded on standard deviation of the compass heading, rate of turning based on differences in compass heading between the first and second halves of each ensemble, and acceleration based on differences in average position for each third of the ensemble. After sensitivity studies, ensembles were accepted when the standard deviation of heading was <5° over the 5-min ensemble, acceleration was <10 cm s^{-1} min^{-1}, and turning rate was <2° min^{-1}.

To calibrate the data from the shipboard ADCP, bottom-tracking calibration runs were made in both 1997 and 1998, yielding a misalignment angle of 0.4° and a speed bias of 12.4 cm s^{-1}. For the 1995 towed ADCP system, calibration is more difficult because the compass bias may be a function of heading. However, the bathymetry of the region is naturally suited to the collection of bottom-tracking data at a variety of headings. Define θ as the true direction (°T) the ship travels over the solid earth; θ_{BT} is the direction of ship velocity estimated from bottom-tracking pings and θ_{GPS} is the direction based on GPS satellite data. The misalignment angle is defined as $\alpha = \theta_{BT} - \theta_{GPS}$, where α is calculated as a function of ADCP compass heading and the results least squares fit using the functional recommended by *Joyce* [1989] and *Münchow et al*. [1995]:

$$\alpha = a + b \cos \theta + c \sin \theta + d \cos 2\theta + e \sin 2\theta.$$

To construct this empirical calibration curve (Table 1), bottom-tracking 5-min ensembles, screened by computer for acceleration and turning, were carefully hand-examined. Ensembles were rejected when a more subtle trend of acceleration or turning was apparent from the surrounding ensemble-average heading and bottom track speed data. Segments of at least three ensembles or 15 min of strait steaming were then averaged into segment-average values of GPS and bottom track velocity.

The raw ping data were then calibrated, rescreened, and reaveraged into 5-min ensembles. Sections were defined for the repeat surveys in the five main passages, and screened, tidally corrected (as detailed in section 2.3) ensembles were averaged into bins 0.025° (~2.75 km) in width across the strait and 10 m in depth, with the shallowest bin located at 15–25 m, depending on the particular instrument used.

Surveys in all 3 years had to contend with GPS navigation data affected by "selective availability," the intentional degradation of the GPS signal by the U.S. Department of Defense. We explored correction of the navigation data using wide-area GPS data from the Canadian Geodetic Survey. However, in a test calculation using the ADCP data from Lombok Strait, 1995, the standard deviation for the screened 5-min ensemble averages was not significantly improved. Subsequently, given the larger errors in estimating the tidal velocity associated with short survey periods, as detailed in section 2.3, we abandoned this postcruise correction of the navigation data.

2.3. Tidal Correction of ADCP Data

Tidal flows in the various straits can be quite strong and represent the greatest source of error for determining the geostrophic flow from our ADCP and pressure gauge measurements. The region is not well-suited to using methods where a grid-like survey pattern is leveraged to provide the spatial and temporal structure of the tides [e.g., *Candela et al*., 1992]; our cruise track is spread out linearly along the archipelago, a region with substantial regional tidal variability due to incident waves from both the Indian and Pacific Oceans [*Wyrtki*, 1961; *Hatayama et al*., 1996]. However, numerous repeat crossings of each strait were made as time allowed in order to directly resolve as many frequencies as possible of the tidal cycle (see Tables 2–6). *Münchow et al*. [1992] directly estimated the M_2 tide with nine repeat ADCP transects taken over 24 hours across the mouth of the Delaware Bay, successfully resolving tidal current speeds of 40–90 cm s^{-1}, and subtidal current speeds of 5–15 cm s^{-1}. Their repeat ADCP section passed through the location of a current meter, allowing direct comparison with a longer (5-month) time series. The 24-hour ADCP survey overestimated the M_2 amplitude by about 15% because of unresolved tidal constituents; phase agreed to within 50 min. Of importance to our study, *Münchow et al*. [1992] found close agreement in subtidal velocity structure using either short-term ADCP or long-term current meter data to remove the tidal velocity.

Our application here is similar to that of *Münchow et al*. [1992], although we average spatially across the strait to estimate a single tidal velocity profile. In each vertical bin we fit a mean velocity plus semidiurnal and diurnal harmonics to the ensemble-averaged ADCP data, regardless of cross-strait position. By representing the tide with a single profile we make an assumption that there is no aliasing of cross-stream tidal structure into the subtidal flow by the sampling pattern. Obviously, for a sufficiently large number of section repeats, aliasing is usually minimized automatically. The spatial deviation from the average tidal profile will average to zero for sampling that is evenly distributed over tidal phase at a given location. However, sampling pathologies are possible. For example, if the strait crossing time is equal to half the semidiurnal period, then cross-stream structure and temporal tidal variation will be inextricably aliased. Computing a tidal fit at each lateral position in the strait will not ameliorate sampling problems of this nature. However, the use of all the data to estimate a single tidal profile provides a first cut at the tidal velocity during sampling gaps at locations with sparse or pathological sampling, allowing for an estimate of subtidal velocity, albeit one which needs to be considered in light of possible aliasing of cross-stream tidal structure. The magnitude of the problem in a particular situation can be assessed through the correlation between cross-stream position and tidal phase as indicated by the pressure gauge data. In the following, this relationship was carefully examined before drawing conclusions about features

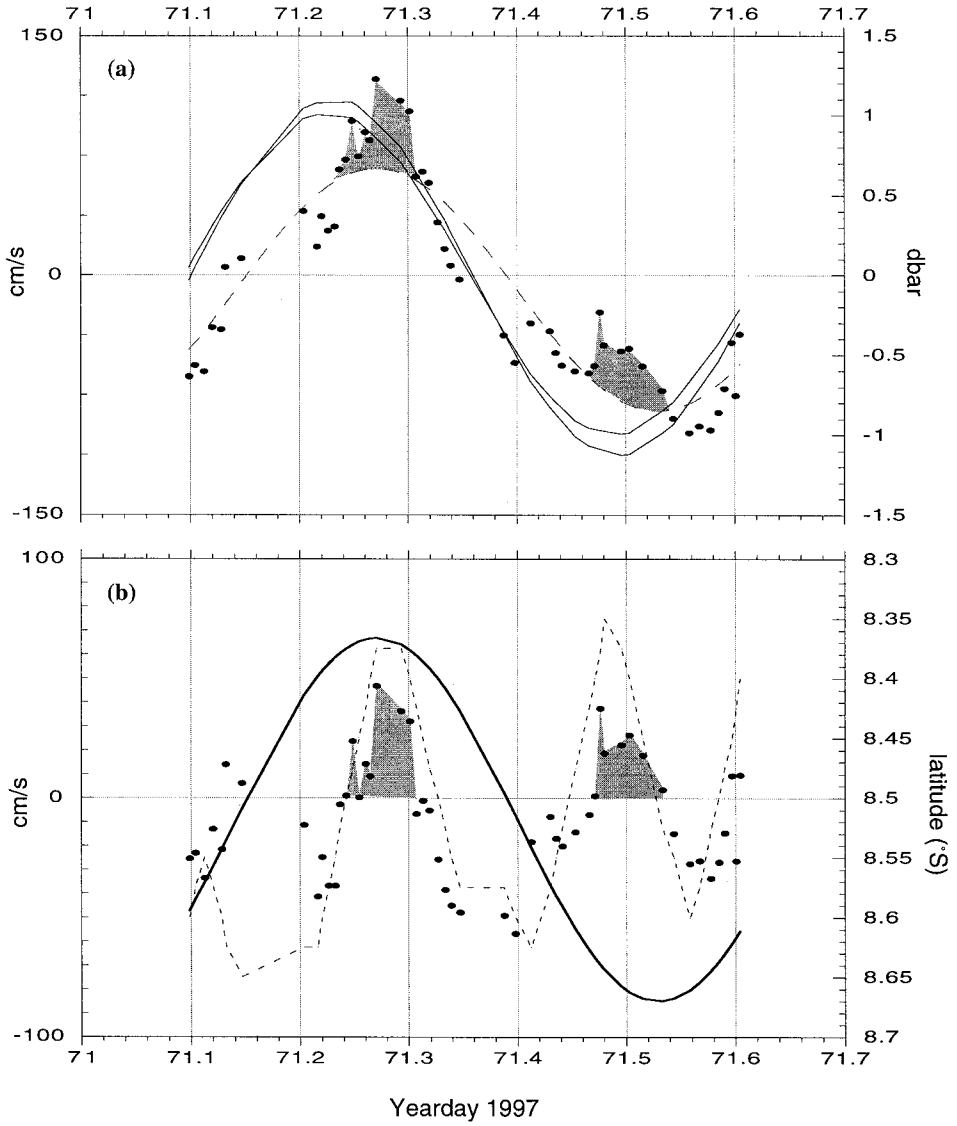

Figure 2. Tidal correction in Ombai Strait, March 1997. (a) Pressure, north and south gauges (solid), 45-m along-strait velocity from ADCP ensembles (dots), and tidal fit to ADCP velocity using a semidiurnal harmonic (dashed). (b) Tidal fit as in Figure 2a (solid), ADCP velocities with tidal fit removed (dots), and across-strait position (latitude, dashed). Negative values represent westward flow toward the Indian Ocean.

of the subtidal flow. Reported error bars, which reflect the variance about the estimate of subtidal velocity from each of our transects, dwarf the uncertainties due to ping-to-ping noise and navigation errors in the ensemble averages themselves.

An example of the tidal correction for one of the more undersampled cases is shown in Figure 2. The March 1997 survey of Ombai Strait, which has the strongest tidal flows of all our five straits, consisted of five crossings over 13 hours, barely spanning one semidiurnal tidal cycle. Thus we fit the data with only the semidiurnal harmonic. However, as is apparent from an examination of the ADCP data corrected for the tide (the dots in Figure 2b) and the ship's position in the strait (dashed line in Figure 2b), substantial subtidal cross-strait structure emerges, even with sampling of suboptimal duration. For example, we found an eastward flowing subtidal current (indicated by shading in Figure 2) in the northern half of the strait of similar magnitude at both peak tidal ebb and at peak flood, confirming that this feature (discussed in greater detail in sections 3c and 5a) is not likely to be explained by aliasing of the cross-stream tidal structure.

By way of contrast, the March 1998 survey of Ombai Strait consisted of 34 crossings spanning nearly 4 days (88 hours). This high sampling density allowed us to directly test the use of a single cross-strait tidal velocity profile. Figure 3 shows the along-strait velocity corrected for the tide as described above, overlaid with a section where the tidal fit was made at each depth and latitude bin independently (where data allowed). While there are quantitative differences apparent in Figure 3, it is clear that correction with a cross-strait average tidal profile effectively captures the overall structure and transport through Ombai Strait during March 1998; use of the cross-strait average tidal profile versus tidal correction in each lateral and vertical bin results in only a 0.1-Sv transport difference.

Of the 12 ADCP survey periods in the Indonesian outflow straits used in the following tidal analysis, four shorter duration surveys were fit using only a semidiurnal harmonic. These

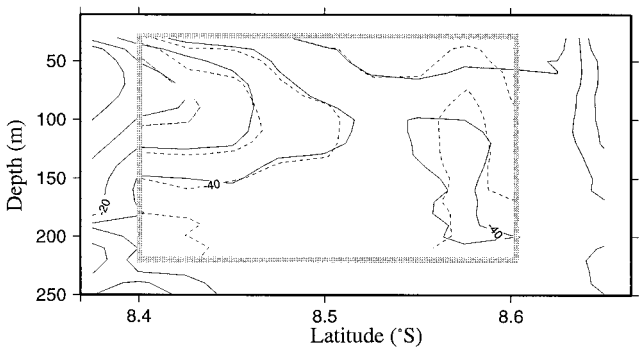

Figure 3. Tidally corrected, along-strait velocity sections across Ombai Strait, March 1998, using two different methods of tidal correction. The solid lines show results that use an average tidal profile (tidal velocity of $f(z)$ only). The dashed lines show results that use an independent tidal correction for each lateral and vertical bin (tidal velocity of $f(y, z)$). The domain of the second tidal correction is substantially reduced because of requirements on data density for a meaningful fit. The box shows the subdomain where both fits have been applied.

occurred during March 1997 in Ombai Strait; December 1995 in Sumba Strait; and December 1995 and March 1997 in Savu/Dao Straits. In addition, acquisition failure during the March 1997 survey of Sumba Strait resulted in a partial single crossing of short duration. The tidal velocity for this survey was estimated using the semidiurnal and diurnal harmonics from the March 1998 survey, with amplitude and phase scaled using the ratio of pressure harmonic analysis parameters during each survey period. Although there may be significant error associated with proportional scaling of velocity and pressure, the observed flow structure is similar to the March 1998 survey and reinforces the conclusions drawn. Because of its great width, aliasing of cross-stream structure is also likely to be a significant problem in Savu/Dao Straits, and we are careful to avoid overreliance on the accuracy of that subtidal flow picture. With the exception of a single current meter mooring [*Molcard et al*., 1994], direct velocity measurements have not previously been undertaken in Savu/Dao Straits, so we present results here as a useful first look at the flow in that region.

We explored the feasibility of tidal correction using version TPXO.3 of the Indonesian regional tidal solution constrained by TOPEX/Poseidon data [*Egbert et al*., 1994] by comparing tidal model predictions with the observations in Ombai Strait, March 1998. The tidal model predicted a velocity variation that was ~30% of the observed range at 45 m (25 versus 80 cm s^{-1}) and also showed a phase shift of more than 2 hours. In addition, the ADCP data reveal significant depth dependence to the tidal velocity; at 145 m the semidiurnal component amplitude was less than a third of its size at 45 m. We concluded that the regional tidal model cannot represent the details of tidal velocity in the straits with sufficient accuracy to improve the tidal correction calculated with the much higher resolution ADCP sections themselves. We plan to explore whether the tidal model may still be useful in providing larger-scale tidal fields with which to estimate subtidal flow in the broader underway data set.

3. Sections Across the Outflow Straits

Because of the unknown vertical placement of the pressure gauges with respect to the geoid, pressure differences across the strait can only yield information about the variability of geostrophic flow. The repeat ADCP transects were included in the experiment design to provide direct velocity measurements with which to "level" the pressure difference time series and provide an estimate of the time-average flow. However, since they are also the first realizations of the full, cross-strait velocity structure in the outflow channels, they provide an interesting glimpse at the vertical and lateral structure of the subtidal flow. Although the ADCP typically only measures the flow in the upper 200 m, this limitation is well-matched to the strongly surface-intensified flow structure associated with the through flow as it exits into the Indian Ocean. Of course, the ADCP sections presented here represent one-time snapshots of the velocity structure in the outflow straits. Given the expected high level of variability that characterizes the region [*Meyers*, 1996], this section should be regarded as an exploratory description of the subtidal flow structure that will require the collection of much more data over a longer period of time to substantiate. Nonetheless, the ADCP sections presented here suggest quasi-permanent features that may help to guide the design of future observational programs in the region.

3.1. Lombok Strait

In Lombok Strait (Table 2 and Figure 4), there is some ambiguity in defining the cross-strait direction since the ADCP survey line between the pressure gauges (along 79°T) did not cross isobaths in a precisely perpendicular sense (closer to 99°T); an exploration of values for cross-strait direction within

Table 2. Summary of ADCP Transects Across Lombok Strait[a]

	Dec. 1995	March 1997	March 1998
Number of transects	8	17	20
Temporal span, hours	19	41	42
Number of harmonics in fit	2	2	2
50-m tidal amplitude, cm s^{-1}			
Semidiurnal	36.4	5.4	8.6
Diurnal	24.3	12.7	15.7
Average along-strait velocity, cm s^{-1}			
At 25 m	59.0 ± 14.5	−73.6 ± 19.7	−71.8 ± 16.7
At 145 m	−16.4 ± 12.0	−59.2 ± 8.9	−19.3 ± 9.9
Transport, Sv			
0–100	1.2 ± 0.5	−1.9 ± 0.3	−1.5 ± 0.3
0–200	0.9 ± 0.9	−3.4 ± 0.7	−2.3 ± 0.7

[a]Negative values indicate flow toward the Indian Ocean. Width is 37 km, and angle is 79.0°T.

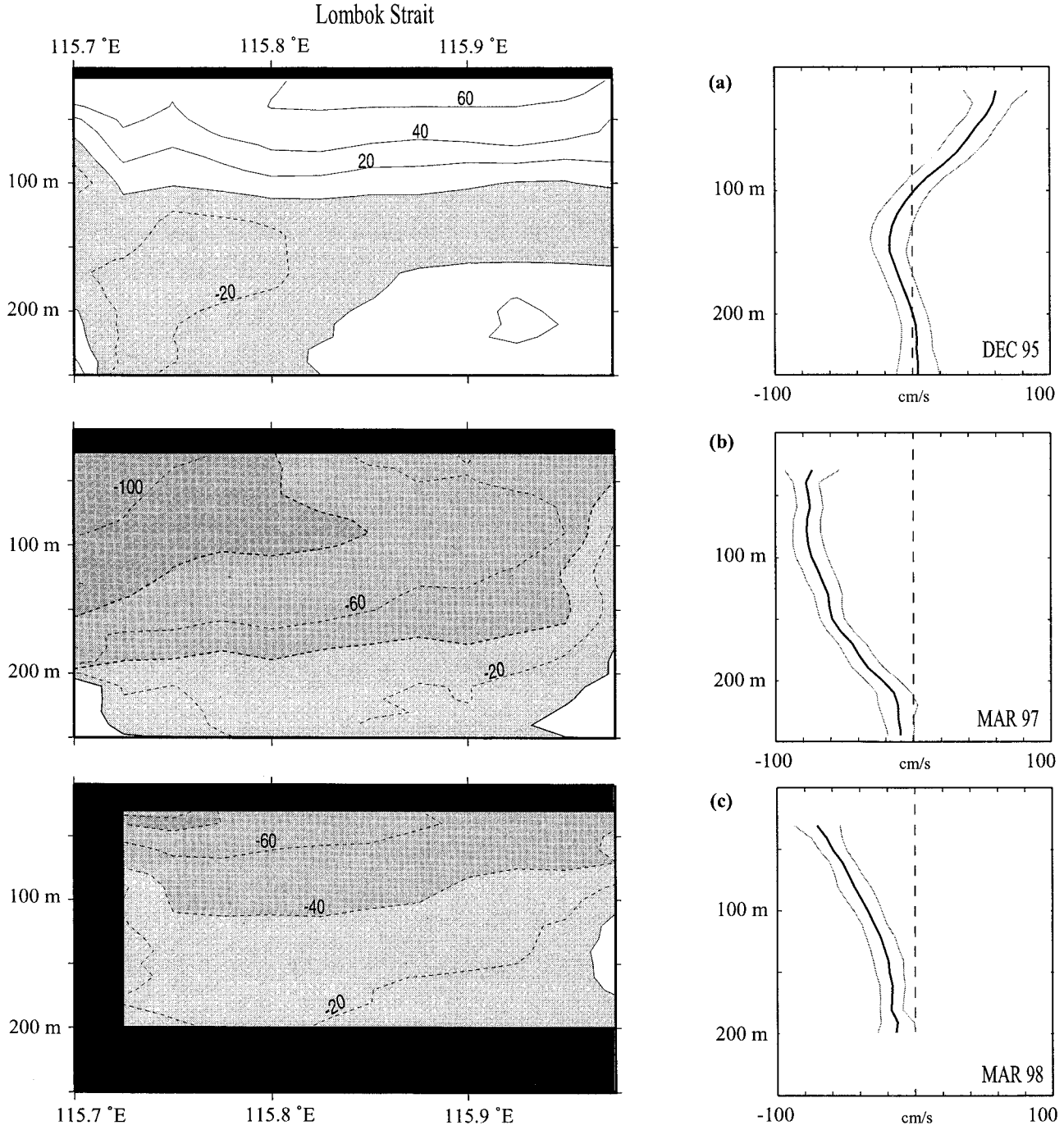

Figure 4. (left) Lombok Strait tidally corrected along-strait velocity sections (contour interval is 20 cm s^{-1}; negative values, shaded, are directed toward the Indian Ocean) and (right) laterally averaged along-strait velocity profiles, with error bars shown by gray lines, for (a) December 1985, (b) March 1997, and (c) March 1998.

this reasonable range does not affect the overall conclusions substantially, although quantitative details do vary.

Of all the straits, the flow in Lombok Strait is perhaps best documented, largely because of the Lombok Strait Experiment [*Murray and Arief*, 1988; *Murray et al*., 1990; *Arief*, 1992]. Flow through Lombok Strait is restricted by a sill of ~300 m depth at its southern end [*Arief*, 1992]. As reflected in the magnitude of tidal velocities in Table 2, the upstream location of our pressure gauge pair avoids the high tidal current regime near the sill with observed speeds of up to 3 m s^{-1} [*Murray et al*., 1990]. The northern pair of moored current meters during the Lombok Strait Experiment were located upstream of the sill a similar distance to our pressure gauges. *Murray and Arief* [1988] documented episodes of northward flow (and thus against the mean through flow direction) at the northern instruments, up to 75 cm s^{-1} in their 25-m current meter. They explained these events as being due to Ekman transport toward or away from the coast associated with cyclones passing

Table 3. Summary of ADCP Transects Across Sumba Strait[a]

	Dec. 1995	March 1997	March 1998
Number of transects	3	1/2	10
Temporal span, hours	34.8	2	36
Number of tidal harmonics	1	[b]	2
50-m tidal amplitude, cm s^{-1}			
Semidiurnal	6.8	3.6	15.4
Diurnal	NA	5.2	1.5
Average along-strait velocity, cm s^{-1}			
At 25 m	99.3 ± 9.4	NA	−10.3 ± 17.4
At 145 m	3.8 ± 5.8	−8.8	−19.8 ± 17.2
Transport, Sv			
0–100	5.7 ± 0.6	−1.6	−0.9 ± 0.8
0–200	6.0 ± 1.1	−3.7	−2.5 ± 1.8

[a]Negative values indicate flow toward the Indian Ocean. Width is 71 km, and angle is 158°T. NA indicates not available.
[b]Extrapolated from 1998 tidal fit as described in the text.

westward through the center of the Indo-Australian Basin. These events may cause a temporary reversal of the along-strait shallow pressure gradient by raising sea level on the Indian Ocean side. Sea level at the southern end of Lombok Strait is also remotely forced by Kelvin waves along the eastern Indian Ocean boundary, particularly during the monsoon transition periods (November/December and April/May) when equatorial Indian Ocean westerly wind events are most prominent [*Clarke and Liu*, 1993; *Chong et al*., 2000; *Sprintall et al*., 1999, 2000; Potemra et al., submitted manuscript, 2001]. All three of our ADCP surveys in Lombok Strait occurred during the northwest monsoon (December–March). Transports observed by *Murray and Arief* [1988] during this part of the year were typically southward 1 Sv or less, compared to the 4-Sv southward maximum they observed during the southeast monsoon in August. The 1985 annual mean transport reported was 1.7 Sv southward [*Murray and Arief*, 1988].

Our three ADCP sections (Figure 4) resolve the upper/lower layer distinction first noted by *Murray and Arief* [1988]. During December 1995, flow in the upper 100 m reversed northward (i.e., was directed away from the Indian Ocean in the opposite sense to the mean throughflow) with speeds intensifying towards the surface to ~60 cm s^{-1}. A deeper layer shows more stable outflow toward the Indian Ocean with velocities of 20–60 cm s^{-1} that decrease to near zero at ~200 m depth.

In all 3 years, outflow to the Indian Ocean is intensified toward the western (Bali) side of the strait. In the March 1997 and 1998 surveys, when the entire water column above 200 m was flowing toward the Indian Ocean, surface velocities exceeded 100 cm s^{-1} near Bali. This cross-strait velocity gradient cannot be due to aliasing of the tidal flow structure. For example, in 1997 the observed range of velocities (prior to removal of the tide), well-distributed with respect to tidal phase over the 41 hours of observation were eastern side, 0 to −70 cm s^{-1}, and western side, −75 to −150 cm s^{-1} (negative values indicate flow toward the Indian Ocean). A comparable difference in total velocity range at either side of the strait was observed in March 1998. This cross-strait velocity structure is also supported by differences between the eastern and western 25-m upstream current meters during the Lombok Strait Experiment in July/August 1985 [*Arief*, 1992]. The oft-cited average transport through Lombok Strait of 1.7 Sv by *Murray and Arief* [1988] was based on an average of the current meter data from either side of the channel, even though the upper layer on the western (Bali) side of the channel was only instrumented after June 1985. Thus their reported transport curve may tend to underestimate the amplitude of the outflow pulse occurring near the end of the southeast monsoon and, consequently, to underestimate the annual average as well.

3.2. Sumba Strait

There are no previous direct measurements of velocity in Sumba Strait (Table 3 and Figure 5). Given the strait's orientation (Figure 1), the usual sense of the through flow in Sumba Strait is westward, toward the Indian Ocean. Our three ADCP snapshots reveal a two-layer vertical structure qualitatively similar to that found in Lombok Strait but differing in detail (Figure 5). Upper layer response to the December 1995 intraseasonal wind event is particularly striking in Sumba Strait, which shows reversed upper layer flow that extends slightly deeper to ~150 m and with eastward velocities close to 1 m s^{-1} (Figure 5). Below this surface layer, flow with speeds of 60–80 cm s^{-1} is directed toward the Indian Ocean.

Lateral structure in Sumba Strait is fairly complex. Outflow in either layer appears to be concentrated in a subsurface layer in the central part of the channel. In addition, during December 1995 the upper layer shows a coastally and surface intensified eastward current near Sumba Island, on the southern side of the channel (Figure 5). In December 1995, while the center of the channel was sampled over the full range of tidal phase, because of ship acceleration near one of the turns, the southern end was only sampled at slack and high tide, and we have some concern about aliasing the tidal structure. However, in March 1998 the data were well distributed with respect to the tidal phase, and the structure shows weakened outflow on the southern side of the channel, supporting the latitudinal velocity gradient seen in 1995. Similarly, in 1995 the northern boundary was only sampled at low tide, and the strong velocity gradient seen between the last two bins at the northern end of the section may again be an artifact of aliasing a coastal tidal stream. There is also indication of an eastward subsurface current, concentrated at 100–200 m depth on the northern boundary of the strait, that is well resolved by the temporal sampling distribution in March 1998. Recall that the ADCP survey in March 1997 consisted of a partial single crossing and that we used the 1998 tidal parameters to estimate the tide. Although the error level is inherently higher, this section also shows a subsurface eastward current.

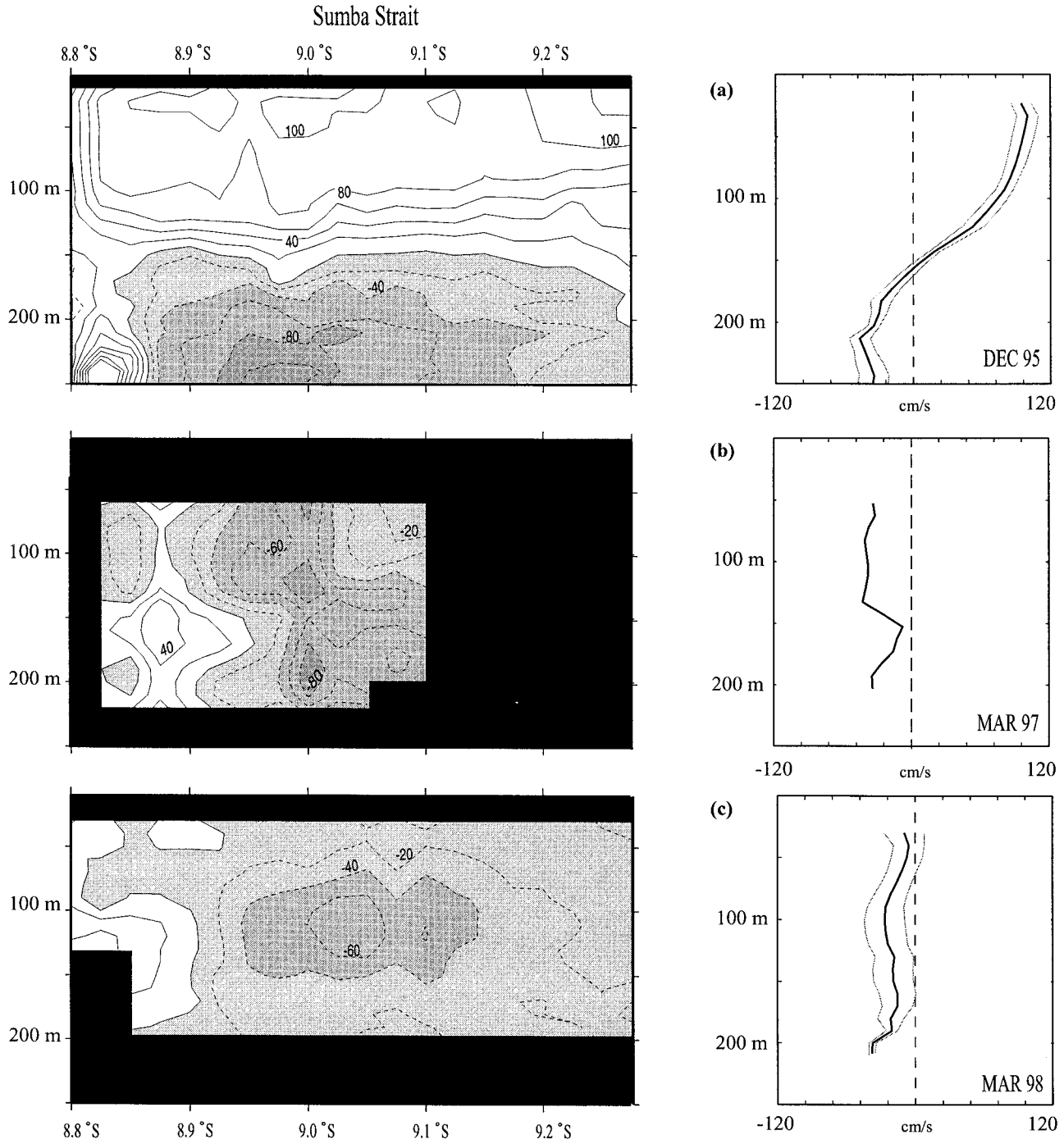

Figure 5. (left) Sumba Strait tidally corrected along-strait velocity sections (contour interval is 20 cm s^{-1}; negative values, shaded, are directed toward the Indian Ocean) and (right) laterally averaged along-strait velocity profiles, with error bars shown by gray lines, for (a) December 1995, (b) March 1997, and (c) March 1998.

Just to the east of the Sumba Strait pressure gauge pair, between the islands of Sumbawa and Komodo, lies Sape Strait (Figure 1). Sape Strait has a relatively small cross section (width ~19 km, sill depth <200 m). Two surveys of this minor strait, made during December 1995 and March 1998, suggest that it may be a significant conduit for flow between the Flores and Savu Seas (Figure 1). Because of time constraints, the ADCP survey in December 1995 was limited to six transects over 9 hours. The subtidal flow (Figure 6) shows surface intensified, northward flow toward the Flores Sea of up to 100 cm s^{-1}, associated with a transport in the upper 150 m of 1.4 ± 0.4 Sv. Thus, about a quarter of the observed eastward flow in the upper layer of Sumba Strait at this time was siphoned off northward through Sape Strait before the balance presumably continued eastward across the ~900-m [*Van Riehl*, 1943] sill between Flores and Sumba Islands and into the Savu Sea (Figure 1). The March 1998 survey consisted of 10 transects over 13.2 hours. During this time, opposing southward flow on

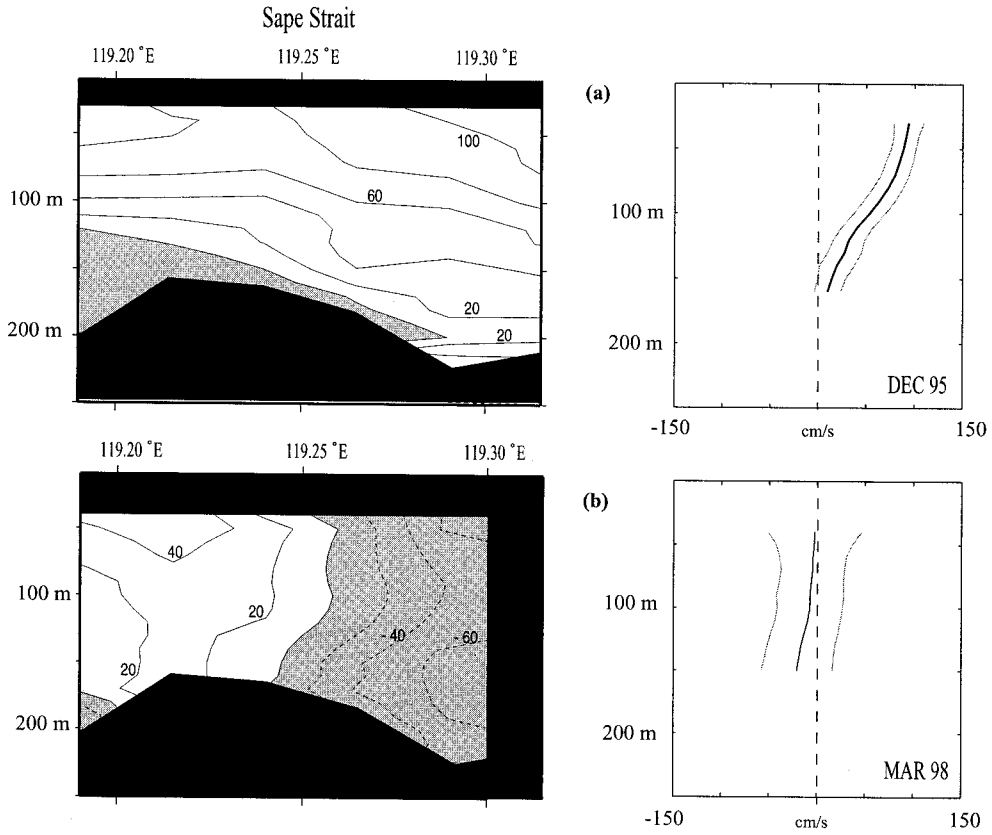

Figure 6. (left) Sape Strait tidally corrected along-strait velocity sections (contour interval is 20 cm s^{-1}; negative values, shaded, are directed toward the Indian Ocean) and (right) laterally averaged along-strait velocity profiles, with error bars shown by gray lines, for (a) December 1995 and (b) March 1998.

the eastern side and northward flow on the western side largely cancelled each other, yielding a total transport of only -0.2 ± 0.1 Sv.

3.3. Ombai Strait

Flow through Ombai Strait (Table 4 and Figure 7) is vertically restricted by sills of ~1000 m depth at the western edge of the Savu Sea at Sumba and Savu/Dao Straits. The deep Savu Sea is in communication with the Banda Sea (Figure 1) to a depth of ~2100 m [*Van Riehl*, 1943], with the choke point occurring ~50 km east of the pressure gauge pair. Unfortunately, we do not have ADCP measurements in Ombai Strait during December 1995, when eastward flow was observed in the upper layer at Sumba Strait (Figure 5). However, the pressure gauge differences indicate eastward flow at the surface during this time. A current meter mooring deployed in December 1995, under the auspices of the Java Australia Dynamics Experiment (JADE), also shows eastward flow of 50–100 cm s^{-1} extending to ~160 m at this time [*Molcard et al.*, 2001]. As we will discuss, the reversed surface flow during December 1995 is most likely due to the seasonal eastward incursion of the South Java Current, associated with the pas-

Table 4. Summary of ADCP Transects Across Ombai Strait[a]

	Dec. 1995	March 1997	March 1998
Number of transects	NA	5	22
Temporal span, hours	NA	13	88
Number of tidal harmonics	NA	1	2
50-m tidal amplitude, cm s^{-1}			
Semidiurnal	NA	71.2	36.7
Diurnal		NA	6.8
Average along-strait velocity, cm s^{-1}			
At 25 m	NA	8.8 ± 15.2	-50.0 ± 18.7
At 145 m		-39.3 ± 24.3	-40.8 ± 17.9
Transport, Sv			
0–100	NA	-0.3 ± 0.4	-0.9 ± 0.5
0–200		-1.8 ± 1.1	-2.2 ± 1.0

[a]Negative values indicate flow toward the Indian Ocean. Width is 35 km, and angle is 180°T. NA indicates not available.

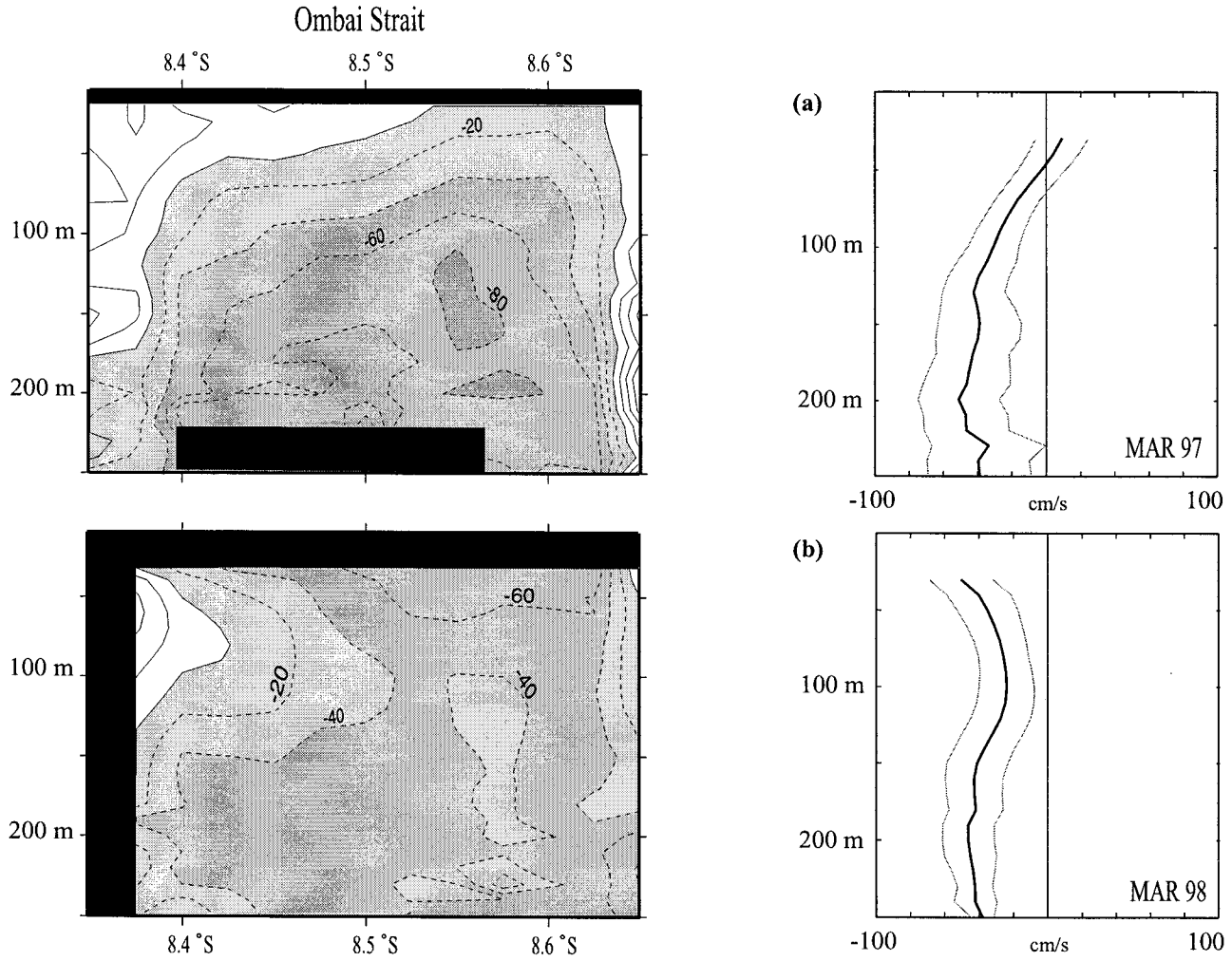

Figure 7. (left) Ombai Strait tidally corrected along-strait velocity sections (contour interval is 20 cm s^{-1}; negative values, shaded, are directed toward the Indian Ocean) and (right) laterally averaged along-strait velocity profiles, with error bars shown by gray lines, for (a) March 1997 and (b) March 1998.

sage of the downwelling coastal Kelvin wave passing into the Savu Sea and on through Ombai Strait (Potemra et al., submitted manuscript, 2001). Indeed, cross correlations of the pressure gauge time series during December 1995 show the eastward propagation from Bali to Sumbawa (northern Sumba Strait) to the Ombai Strait gauges, with a speed of roughly 2.5 m s^{-1}, commensurate with linear wave theory [*Chong et al*., 2000].

It appears that Ombai Strait may well have a two-layer vertical structure comparable to those of Lombok and Sumba Straits, with the upper layer flow displaying episodic reversals. An empirical orthogonal function (EOF) decomposition of both the mooring data [*Molcard et al*., 2001] and POCM model output (Potemra et al., submitted manuscript, 2001) in Ombai Strait finds a first mode that contains most of the energy characterized by slab-like flow in the upper 100 m (200 m in the model) decaying to zero at ~400 m, with weak annual variability. The second mode is more baroclinic, changing sign at 70 m (100 m in the model) and extending to ~600 m depth. This second mode has a strong semiannual response, with maxima occurring in May and December in accordance with the expected semiannual passage of Kelvin waves.

During March 1997 and March 1998, while most of Ombai Strait showed the strong westward through flow, eastward flow was observed in both years at the Alor (northern) side of the channel (Figure 7). Careful consideration outlined earlier in relation to Figure 2 rules out an explanation due to aliasing of the cross-strait tidal structure. Considering the existence of an analogous feature during the same survey periods in Sumba Strait (Figure 5), we speculate that this feature is an extension of the South Java Current through Ombai Strait into the Banda Sea.

3.4. Savu and Dao Straits

At 244 km, the combined Savu and Dao Straits (Table 5 and Figure 8) compose the widest of the five passages surveyed (Figure 1). This connection between the Indian Ocean and the Savu Sea is broken midchannel by Savu Island, which was not instrumented with a pressure gauge. Although it is drawn schematically in Figure 1 as passing through the island, the ADCP transects actually arced either north or south of Savu, staying outside the 200-m isobath. The channels east (Dao Strait) and west (Savu Strait) of the island have similar sill depths of ~1100–1200 m [*Van Riehl*, 1943]. Particular caution must be used in interpreting these velocity sections given the combined width of the straits (recall that an average tidal velocity profile

Table 5. Summary of ADCP Transects Across Savu and Dao Straits[a]

	Dec. 1995	March 1997	March 1998
Number of transects	2/3	1	3
Temporal span, hours	11	12	48
Number of tidal harmonics	1	1	2
50-m tidal amplitude, cm s^{-1}			
Semidiurnal	48.9	21.9	34.4
Diurnal	NA	NA	4.9
Average along-strait velocity, cm s^{-1}			
At 25 m	−21.1	−4.3	−8.9 ± 8.2
At 145 m	−14.4	−0.2	2.8 ± 9.1
Transport, Sv			
0–100	−5.3	−2.3	0.0 ± 2.0
0–200	−8.7	−2.5	0.2 ± 3.7

[a]Negative values indicate flow toward the Indian Ocean. Width is 244 km, and angle is 105°T. NA indicates not available.

is removed from all cross-strait bins in both straits), and the high ratio of tidal to subtidal speeds (Table 5). Nonetheless, certain consistent features appear in all three sections. Velocities are smaller than in any of the other passages (Table 5 and Figure 8); however, the weak net transport observed during the ADCP surveys is largely due to cancellation of counterflows in the straits (Figure 9). In particular, there appears to be a persistent northeastward flowing boundary current on the northwest side of Savu Island. Outflow into the Indian Ocean, on the other hand, is concentrated over the deepest parts of the two channels. *Molcard et al*. [1994] observed a similar structure in their 1989–1990 current meter mooring, located at (10°59′S, 121°44′E), about 50 km downstream of the eastern tip of Savu Island, which showed a very weak (2.1 cm s^{-1}) mean outflow (toward the Indian Ocean) only in the shallowest instrument at 90 m depth, with comparably sized mean inflow recorded by all four of the deeper instruments.

3.5. Timor Passage

Because of logistics, we have only one repeat section across Timor Passage (Table 6 and Figure 10), taken in December 1995. The location roughly corresponds to a deep western (~1950 m [*Van Riehl*, 1943]) sill between the Indian Ocean and the Timor Trench, but it is substantially downstream of the primary eastern sill of 1250–1400 m depth, located northeast of Timor Island (Figure 1) [*Van Bennekom*, 1988]. Flow in Timor Passage has been observed previously through current meter deployments and has been shown to host a relatively steady, surface-intensified flow toward the Indian Ocean [*Molcard et al*., 1994, 1996]. Our single ADCP section also shows a surface intensified core of current, moving westward at 30–40 cm s^{-1}, and located over the deepest part of the channel.

The location of the two JADE 1992–1993 moorings are shown by the arrows in Figure 10. *Molcard et al*. [1996] presented two extrapolation schemes: (1) maximal, an average of the two moorings applied to the area between the moorings and tapering to zero on either, side, and (2) minimal, assuming zero flow outside the moorings. The southern side of Timor Channel is more gently sloped than the north side, and the flow structure observed in December 1995 suggests that the high-velocity outflow core may extend over this flank farther to the south than previously believed. If this structure is representative, then even the maximal estimate of *Molcard et al*. [1996] is a lower bound for transport through the channel. The maximal annual-average transport calculated by *Molcard et al*. [1996] for the upper 200 m is −2.4 Sv. Although on the basis of the seasonal cycle observed during JADE [*Molcard et al*., 1994, 1996] we expect a value in December of ~75% of the annual average, the 0–200 m transport in the December 1995 ADCP section is −3.6 Sv (Table 6). This value, roughly double that expected, calls for experiments to better characterize the lateral structure of velocity in Timor Passage and how it varies on a seasonal and interannual basis.

4. Absolute Surface Velocity Time Series of Outflow Strait Through Flow

The repeat ADCP sections provide detailed snapshots of flow within each strait, but they can also be used to level the across-strait pressure differences from the pressure gauge data by invoking geostrophic balance between measured absolute velocity and the observed total sea surface slope. Here we shift the time series of geostrophic flow derived from the pressure gauge differences [*Chong et al*., 2000] along the velocity axis to best fit, in a least squares sense, the laterally averaged ADCP velocity at 25 m (Figure 11). A 24-hour average pressure difference centered on the temporal midpoint of each ADCP survey was used to define points to fit to absolute velocity. Partial crossings of Sumba Strait in March 1997 and of Savu/Dao Straits in December 1995 are thought to bias the cross-strait average because of their truncation and were not used in the fit. Despite the simplified methodology that we employ, the results are supported by the agreement in Figure 11 between the relative velocity changes between cruises as calculated from the pressure gauge data and the absolute lateral-average velocity changes observed with the discrete ADCP cross sections (Figures 4–10).

Chong et al. [2000] presented time series of surface geostrophic velocity from a similar calculation using ADCP data prior to correction for the tidal flow. The temporal variability in these geostrophic velocity time series was described briefly by *Chong et al*. [2000], and their results are obviously not affected by addition of the time-mean flow from ADCP data. However, net transport estimates do depend on a reasonable estimate of tidal velocity. The lateral-average surface velocity in both Lombok and Sumba Straits is not significantly different (given the error bars) with or without tidal correction. By contrast, because of the very strong tidal velocities, Ombai Strait flow structure is significantly impacted. Compared with *Chong et al*. [2000, Table 1], tidal correction in Ombai Strait greatly reduces both the shallow outflow velocity and transport in 1997 and brings the overall change between the 1997 and 1998 ADCP

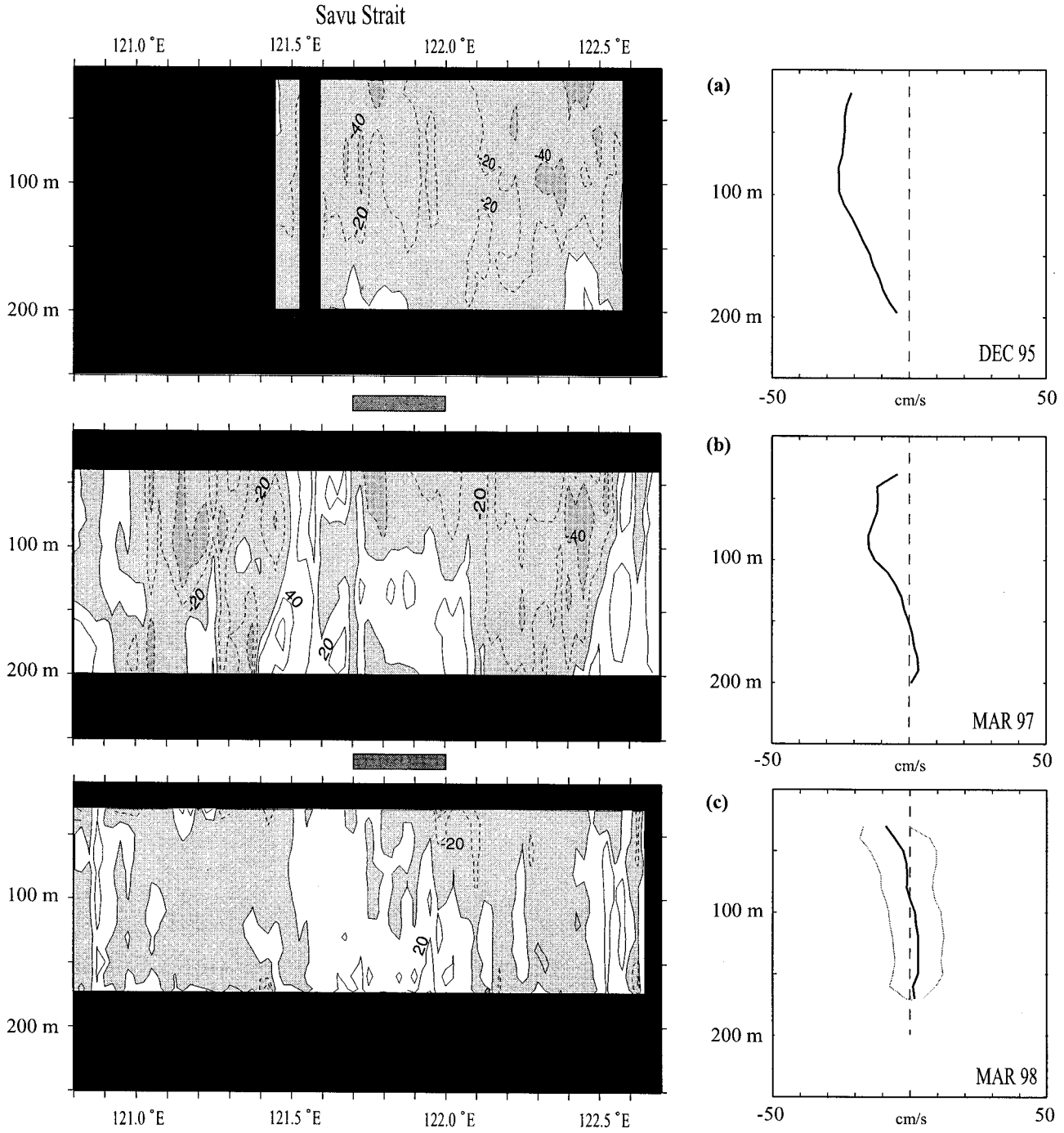

Figure 8. (left) Savu/Dao Straits tidally corrected along-strait velocity sections (contour interval is 20 cm s^{-1}; negative values, shaded, are directed toward the Indian Ocean) and (right) laterally averaged along-strait velocity profiles, with error bars shown by gray lines, for (a) December 1995, (b) March 1997, and (c) March 1998. The shaded bar between each panel indicates the longitudes inside the 200-m isobath off Savu Island.

velocities into much better agreement with the change in geostrophic velocity indicated by the pressure gauges. The agreement gives us increased confidence in both the tidal correction and the essentially geostrophic character of the along-strait flow. Because of low subtidal velocities in Savu/Dao Straits, the final flow field in that passage is also significantly affected by tidal correction; in particular, we now compute substantially less outflow during March 1997, which shifts the estimated mean velocity toward a lower value.

Upper layer (0–100 m) transport values in each strait (Figure 11 and Table 7) have been computed by assuming a linear relationship, $T = a_1V + a_2$, between the laterally averaged 25 m velocity (V) and 0–100 m integrated transport (T) with a regression based on data from the ADCP surveys. In Timor Passage, with only a single ADCP section, we have additionally assumed that the transport is zero when the surface velocity is zero, which probably leads to a modest underestimation of the outflow transport through that strait. The largest source of

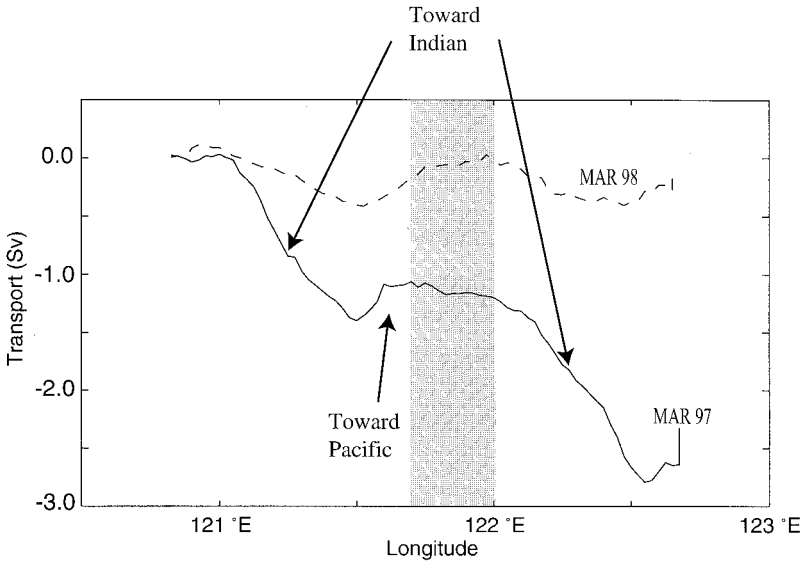

Figure 9. Along-strait transport (0–150 m) integrated from the western end of Savu/Dao Straits to the longitude on the horizontal axis. The solid line is from March 1997, and the dashed line is from March 1998. The shaded area corresponds to the longitudes spanned by the 200-m isobath surrounding Savu Island.

error for the yearly mean transports is the leveling calculation and uncertainties in transports shown in Table 7 reflect the error bars on the ADCP lateral-mean velocity (Tables 2–6) projected onto transport by the regression function. Also shown in Table 7 is an estimation of 0–100 m transport that uses a slab model where the velocity at 25 m is taken to represent the average flow in the layer. As expected, given the surface-intensified nature of flow in this region, the slab estimate is larger than the regression estimate, but except in Timor Passage, the differences do not exceed the error bars.

Modeling the 0–100 m transport as a linear function of the 25-m velocity depends on two assumptions: (1) that the upper 100 m shear is linear and (2) that the variance of velocity at 100 m is much smaller than the variance of velocity at 25 m. These assumptions are both supported to some extent by the available data. As the velocity profiles reveal (Figures 4, 5, 7, 8, and 10), the vertical shear in the upper 100 m is often linear. Profiles that are largely linear in the upper ocean are also observed in the principal modes of variability in Timor [*Molcard et al*., 1996] and Ombai [*Molcard et al*., 2001] Straits. These modes are also strongly surface intensified, with a doubling of amplitude of the principal EOF in both passages from 100 m to the shallowest observation, supportive of the second assumption. Similar behavior is seen in Lombok Strait; although the 100-m level was not instrumented, a strong decrease in overall variation is seen moving from the 25-m to the 200 or 300-m level [*Arief*, 1992]. As discussed in section 2, Potemra et al. (submitted manuscript, 2001) find a strong relationship between upper layer (250 m) transport and sea level difference across the straits in numerical experiments. Although the nature of flow in the passages lends support to our regression approach for the upper 100 m, the two-layer nature of the flow that is revealed by the ADCP sections suggests that using the surface velocity to extrapolate to deeper transport is problematic, and in estimating total transport we will rely on the deep vertical structure revealed by available current meter data.

Further development of this method will require development of a better empirical regression relationship based on simultaneous current meter and pressure gauge data. *Pandoe* [2000] made one such calculation using the 11 months of simultaneous SPGA pressure gauge and JADE current meter

Table 6. Summary of ADCP Transects Across Timor Passage[a]

	Dec. 1995	March 1997	March 1998
Number of transects	4	NA	NA
Temporal span, hours	28	NA	NA
Number of tidal harmonics	2	NA	NA
50-m tidal amplitude, cm s^{-1}			
Semidiurnal	10.8	NA	NA
Diurnal	2.7		
Average along-strait velocity, cm s^{-1}			
At 25 m	-30.8 ± 8.3	NA	NA
At 145 m	-15.9 ± 8.8		
Transport, Sv			
0–100	-2.1 ± 0.7	NA	NA
0–200	-3.6 ± 1.6		

[a]Negative values indicate flow toward the Indian Ocean. Width is 100 km, and angle is 160°T. NA indicates not available.

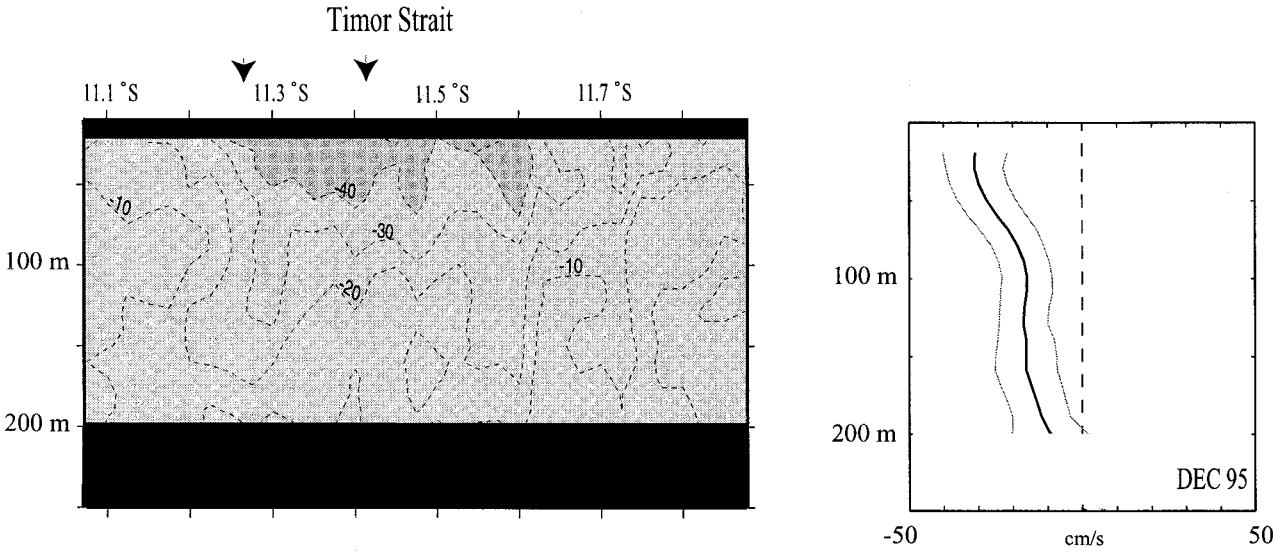

Figure 10. (left) Timor Strait tidally corrected along-strait velocity sections (contour interval is 10 cm s^{-1}; negative values, shaded, are directed toward the Indian Ocean) and (right) laterally averaged along-strait velocity profiles, with error bars shown by gray lines, for December 1995. Arrows show the locations of JADE moorings deployed in 1992–1993 [*Molcard et al*., 1996].

data in Ombai Strait. He regressed the pressure difference data against ADCP velocity at 20-m intervals down to 100 m and then, assuming that the JADE velocity values represented the cross-strait average, used the regression to extend the current time series throughout the SPGA period. The resulting 0–100 m transports were −2.6 Sv (1996) and −2.1 Sv (1997), significantly larger than our estimates in Table 7. Pandoe noted that calculating the transport from the pressure gauge data via the regression overestimated transport by ~20% during the period of overlap. Furthermore, the JADE mooring at 8.5°S is located in the central part of the channel, which will tend to bias this estimate toward higher outflow. *Molcard et al*. [2001] estimate −0.9 to −1.5 Sv as the average transport in the upper 100 m for December 1995 to November 1996 using maximal and minimal assumptions about lateral structure. Although much work remains, such empirical "calibration" of the pressure gauge differences with current meter data, combined with periodic shipboard ADCP surveys to document lateral structure and its variability, may eventually make cross-strait tide gauge data an efficient way to monitor transport through the outflow passages over long timescales.

The net upper layer (0–100 m) transport entering the Indian Ocean (Figure 11) can be constructed in two ways: (1) as the sum of transports through Lombok, Sumba, Savu/Dao, and Timor Straits and (2) as the sum of transports through Lombok, Ombai, and Timor Straits (Table 8). The first estimate directly includes any transport contribution through the numerous shallow straits that lie along the northern edge of Savu Sea (Figure 1), such as Sape Strait, for which we have no pressure gauge time series. As discussed previously, data from the single December 1995 ADCP survey suggest that Sape Strait may at times contribute significantly (~25%) to the flow through the upper layer of Sumba Strait. Finally, because of data gaps that alias the seasonal cycle in the single-year averages, we use the record length average transport through Timor Strait in the summed transport calculations for both years.

The nature of transport through Savu/Dao Straits, which is the sum of alternating currents of only modest magnitude, as well as uncertainty in tidal correction over the large distance between its endpoints, leads to an error level at least double that of any of the other straits. Thus, for future monitoring

Table 7. Upper Layer Regression Coefficients and Transport Estimates[a]

Strait (0–100 m)	a_1, Sv $(cm\ s^{-1})^{-1}$	a_2, Sv	Transport Estimates, Sv			
			1996	1997	1998	Error
Lombok (LBK)	0.022	−0.302	−1.3	−1.3	+0.3	±0.4
Slab			−1.7	−1.7	−0.2	
Sumba (SMB)	0.054	−0.373	+0.3	−1.3	−0.2	±0.7
Slab			+0.9	−1.2	−0.2	
Ombai (OMB)	0.009	−0.428	−0.7	−0.6	···	±0.2
Slab			−1.0	−0.5		
Savu/Dao (SVU)	0.203	−0.24	−0.2	+0.1	···	±1.6
Slab			+0.1	+0.4		
Timor (TMR)	0.067	0.0	−0.9	−1.2	−1.4	±0.6
Slab			−1.4	−2.1	−2.3	

[a]Negative values indicate flow toward the Indian Ocean.

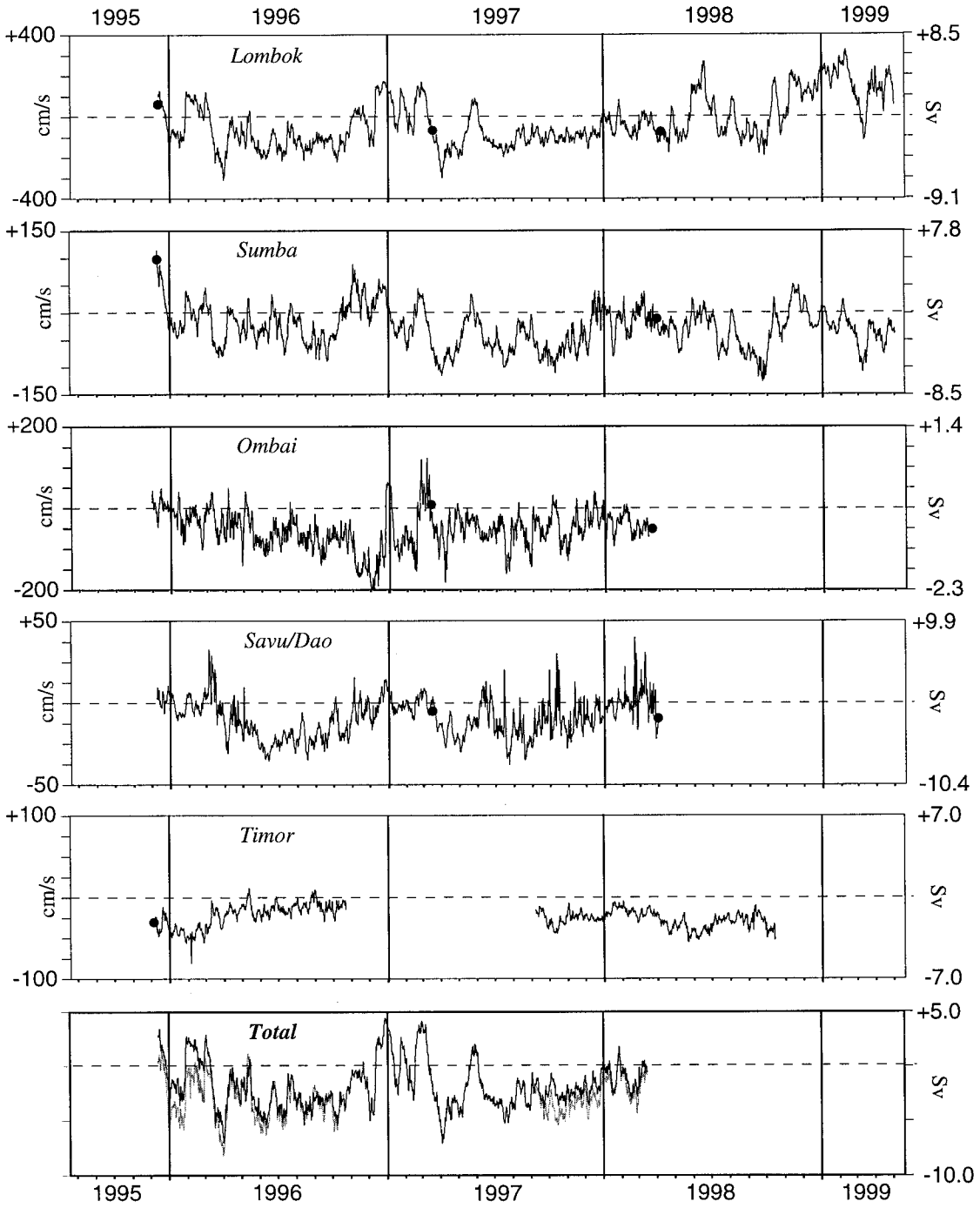

Figure 11. Time series of 25-m along-strait geostrophic velocity and estimated upper layer (0–100 m) transport for each of the straits. The total is two transport sums: Lombok plus Ombai (solid) and Lombok plus Ombai plus Timor (shaded). Note that the velocity and transport scales vary.

purposes the recommended strategy is to directly measure or index flow through Lombok, Ombai, and Timor Straits. In fact, the total upper layer transport constructed from these three straits tends to covary with Lombok Strait transport, with $R^2 = 0.80$, suggesting an important role for this relatively easy to measure location in future long-term monitoring efforts. Part of the reason is that although its temporal character is quite different, the upper hundred meters of Ombai Strait hosts about half the transport in the upper layer of Lombok Strait. In addition, transport estimation from tide gauges may be inaccurate for the deeper Ombai Strait. Also, although Timor Passage has a mean upper layer through flow comparable in magnitude to that found in Lombok Strait, it is significantly less variable (Lombok σ = 2.6 Sv, Timor σ = 0.9 Sv.)

Because of our concerns about the validity of extrapolating the shallow pressure differences to depths >100 m we use historical moored measurements that resolve the vertical structure to estimate total, depth-integrated transport through the outflow straits. In Timor Passage the transport versus depth

profiles of *Molcard et al*. [1996] show that the upper 100 m carried about one third of the total transport (5.3 Sv) for the time period March 1992 to April 1993. In Ombai Strait, *Molcard et al*. [2001] find that the upper 100 m carried about one quarter of the 0–1200 m transport (5 Sv) for the time period November 1995 to November 1996. In Lombok Strait, controlled by a much shallower sill (~300 m), the upper 100 m carried about half the total transport (Table 2) [*Murray and Arief*, 1988]. We assume that these relationships between upper layer and depth-integrated transport are temporally invariant and use them to estimate 2-year (1996–1997) average transport values (Table 9). The total through flow of -8.4 ± 3.4 Sv estimated in this way is consistent with other recent measurements both upstream and downstream of the outflow straits, given the error bars. *Molcard et al*. [2001] sum the transports estimated from the temporally dislocated current meter experiments in Lombok (1985), Ombai (1996), and Timor (1992) Straits to arrive at a total through flow of -11.2 ± 3 Sv into the Indian Ocean. Farther downstream, the long-term (1986–1999) mean geostrophic transport estimated from expendable bathythermograph (XBT) data through the World Ocean Circulation Experiment (WOCE)-IX1 line between Australia and the western tip of Java is -4.2 to -6.7 Sv (depending on reference level between 400 and 700 m) (S. Wijffels and G. Meyers, personal communication, 2000). The transport they obtain for the comparable time period 1995–1998 is -3.7 to -6.1 Sv. Farther upstream, *Gordon et al*. [1999] report a flow of -9.3 ± 2.5 Sv entering the Indonesian seas from the Pacific through Makassar Strait for a single year (1997).

5. Further Discussion

5.1. Eastward Flow Along the Northern Boundary of the Indo-Australian Basin

The South Java Current is a periodic eastward current along the coast south of Sumatra and Java. Ship drift data compiled by the Royal Netherlands Meteorological Institute reveals an annually modulated flow [*Quadfasel and Cresswell*, 1992]. Eastward flow, 20–30 cm s^{-1} in strength, all along the Java-Bali-Sumbawa-Sumba portion of the coastline (Figure 1) begins in October–November. A reversal to westward flow occurs between February and May, with the easternmost portion of the coastline off Sumba reversing earlier than the more westward potion off Java. At the western tip of Java, semiannual variations are observed in a repeat XBT section with peak eastward flows of 4–6 Sv (0–400 m) centered temporally around the monsoon transitions in March and November [*Meyers et al*., 1995]. At other times of the year the coastal flow in the South Java Current is considered to be part of the westward flowing South Equatorial Current [*Meyers et al*., 1995].

Eastward flowing boundary currents, against the prevailing westward through flow from the Banda Sea into the Indo-Australian Basin, were observed along the northern boundary in both Sumba and Ombai Straits in the ADCP sections in March 1997 and March 1998. The strongest current in Sumba Strait is a subsurface feature, centered at a depth of 100–200 m, while in Ombai Strait the eastward current is found from the surface to a depth of ~150 m. The December 1995 ADCP section in Sumba Strait shows eastward flow across the entire width of the strait, extending to a depth of ~150 m (Figure 5), some of which subsequently passes northward through Sape Strait (Figure 6), with the remainder flowing across the Savu Sea and past the mooring in the center of Ombai Strait [*Molcard et al*., 2001]. These flow features are most likely a signature of the South Java Current extending eastward through Ombai Strait to the Banda Sea. Consistent with this hypothesis, three of five surface drifters deployed in the central Indo-Australian Basin near 110°E in November 1993 moved northeastward into the Savu Sea early the following year, with one surviving drifter continuing through Ombai Strait into the Banda Sea [*Michida and Yoritaka*, 1996]. During the SPGA experiment, a current meter mooring was deployed on the shelf at 200 m depth south of central Java with instruments at 55, 115, and 175 m. Wind vectors from nearby Cilacap suggest that in March 1997 the southeast monsoon was well established over Java. Velocities in the top two instruments of the mooring were generally westward. In late April/early May 1997, velocities in the top two instruments of the mooring displayed a brief but striking reversal to eastward flow associated with a coastal Kelvin wave propagating from the equatorial Indian Ocean [*Sprintall et al*., 1999]. Interestingly, flow in the 175-m instrument was weaker (10–20 cm s^{-1}) but persistently eastward. As *Quadfasel and Cresswell* [1992] note, unlike the November monsoon transition, during boreal spring the remotely forced semiannual coastal Kelvin wave works against the local boundary current response to the onset of the regional easterly winds. This may make this phase of the South Java Current annual cycle more variable in general. Further work that fully defines the South Java Current along the Indonesian waveguide between Sumatra and the Lesser Sunda Islands is required to fully characterize the transport, seasonal cycle, and properties of outflow into the Indian Ocean.

Table 8. Yearly Average Upper Layer Transport Sums[a]

Summed Straits (0–100 m)	1996	1997	Error
LBK + OMB	−2.1	−1.9	±0.5
LBK + OMB + TMR	−3.2	−3.0	±1.1
LBK + SMB + SVU	−1.2	−2.5	±2.7
LBK + SMB + SVU + TMR	−2.3	−3.6	±3.3

[a]Negative values indicate flow toward the Indian Ocean. Transport in Sv.

Table 9. Two-year (1996–1997) Estimated Total Transport[a]

Total Transport (Depth-Integrated)	Average, Sv	Error, Sv
Lombok Strait	−2.6	±0.8
Ombai Strait	−2.6	±0.8
Timor Passage	−3.2	±1.8
Total	−8.4	±3.4

[a]Negative values indicate flow toward the Indian Ocean.

5.2. Transport Timing Differences Among the Outflow Straits and Across the Banda Sea

In all the time series of Figure 11 the most striking feature is the strong intraseasonal variability (for further discussion, see *Chong et al*. [2000] and Potemra et al. (submitted manuscript, 2001). On longer timescales the upper layers of Lombok, Sumba, and Savu/Dao Straits (Figure 11) all show the expected annual cycle of maximum through flow in the southeast monsoon during boreal summer [*Wyrtki*, 1987]. In Ombai

Strait the seasonal cycle is not as apparent (although the time series is too short to be conclusive). In fact, we observe maximum outflow in Ombai Strait during November/December 1996 when transport in the other straits is minimal. Although gappy, the Timor Passage time series also has a different character than the other straits, with unexpected maximal through flow during the northwest monsoon of 1995–1996, a time when the other straits showed strong reversals of upper layer flow directed away from the Indian Ocean.

Our time series of upper ocean through flow is also quite different from the recent Makassar Strait record of flow from the Pacific Ocean toward the Banda Sea, which shows little evidence of an annual cycle. *Gordon et al*. [1999] measure high (~15 Sv) through flow in Makassar Strait from December 1996 to August 1997, except for a short interruption in May–June 1997 linked to the Indian Ocean Kelvin wave event also seen in the South Java Current mooring, as noted above [*Sprintall et al*., 1999, 2000], and in the shallow pressure gauge array (Potemra et al., submitted manuscript, 2001). Over the next 4 months from September through December 1997, transport through Makassar Strait decreased to low values (0–5 Sv) that persisted through the northwest monsoon ending in March 1998, at which point transport increased again. Our time series of net upper layer flow entering the Indian Ocean (Figure 11) shows minimum transport at the same time that the Makassar Strait inflow is weak from November 1997 to March 1998; in the outflow straits, minimal flow at this time is the expected seasonal response to the northwest monsoon [*Wyrtki*, 1987]. However, during the northwest monsoon of 1996–1997, transport through Makassar Strait into the interior Indonesian seas was maximal, whereas flow leaving the interior seas for the Indian Ocean was once again minimal. *Gordon et al*. [1999] discuss the predominantly interannual variation seen in the Makassar Strait record as a straightforward response to the lowering of sea level in the western Pacific during the strong 1997–1998 El Niño event that occurred during the deployment period. Currently, we have only records past March 1998 in Lombok and Sumba Straits, but the ENSO response at the outflow straits appears to be, not surprisingly, modulated by events in the Indian Ocean and along the coastal waveguide. Flow through these two straits into the Indian Ocean was greater in November–February 1997/1998 than during the comparable period in 1996/1997, most likely associated with a shift in the Walker circulation in the Indian Ocean that resulted in easterly anomalies along the equator and depressed sea level along the coastal waveguide [*Yu and Rienecker*, 1999]. It is during the second half of 1998 and early 1999 that through flow in Lombok Strait is weakened, with no clear signal in Sumba Strait. Thus the through flow as it enters the Indian Ocean, at least in the upper layer, appears to have a complex relationship to Pacific ENSO forcing, which likely involves the interplay of Banda Sea storage, local forcing, and remote forcing of sea level from the equatorial Indian Ocean.

Part of the apparent differences in timing of transport between the Makassar Strait inflow and Lesser Sunda outflow passages may be due to the nature of the measurements. Because of failure of the upward looking ADCPs, the Makassar Strait transport estimates are based on data below ~200 m and thus may be biased toward the characteristics of the deeper through flow. On the other hand, our SPGA measurements are biased toward the characteristics of the upper through flow. As detailed by Potemra et al. (submitted manuscript, 2001), the inherent timescale of the through flow variations may increase with depth such that the interannual character of the Makassar measurements simply reflects the sampling bias in those deeper measurements. Only Ombai Strait shows a temporal variation similar to the Makassar record.

Because of the possibility of different sampling biases between the recent measurements in the inflow and outflow straits, we cannot unambiguously document transport phase differences across the Banda Sea; simultaneous measurements over comparable depth ranges are required. However, such transport imbalances are not unreasonable given the interplay of Pacific and Indian Ocean forcing on a multitude of timescales, with different balances of forcing factors controlling dynamically distinct regions throughout the archipelago (Potemra et al., submitted manuscript, 2001). Moreover, phase differences of comparable size emerge from the observations of other subbasins in this area where the vertical distribution of the data is directly comparable. For example, in their analysis of repeat XBT sections, *Meyers et al*. [1995] find that the upper Indo-Australian Basin (see Figure 1), bounded on the east by Sumba and Timor Islands and to the west by the ship track between western Java and Western Australia, absorbs a 10-Sv seasonal transport imbalance which they show to be consistent with average depth changes of the 20°C isotherm. *Bray et al*. [1996] extend the calculation to show a consistent sea level anomaly of the opposite sign, as expected. Further, the SPGA time series at Ombai, Sumba, and Savu/Dao Straits suggest substantial seasonal imbalance in the Savu Sea as well. Transports through these three straits balance over the entire 1996–1997 time period to within 0.12 Sv. However, the data indicate a significant seasonal transport imbalance of amplitude ~5 ± 3.5 Sv (allowing for a 1-Sv uncertainty due to the contribution of Sape Strait), with the upper layer draining during the southeast monsoon and filling up during the northwest monsoon.

Timing differences in upper layer transport across the Banda Sea have the potential to significantly impact upper layer heat content. We performed a simple calculation to assess the impact of the observed transport imbalances. We assume isopycnal flow and allow the difference in phase between inflow and outflow to change the thermocline stratification by filling and draining isopycnal layers in a basin the size of the Banda Sea. An imposed transport imbalance of 5 Sv on seasonal to interannual timescales, distributed linearly over the top 200 m and initialized with the average Snellius Makassar Strait temperature stratification [*Hautala et al*., 1996], affects the temperature at thermocline depths by ~5°C. Although more realistic models that include mixed-layer coupling are required, the simple calculation suggests that convergences and divergences of this magnitude can have a substantial impact on thermocline stratification and thus may also affect sea surface temperature by changing the temperature of water entraining into the mixed layer.

The suggested mechanism is not without precedent. In the Tasman Sea, *Sprintall et al*. [1995] analyzed a seasonal transport imbalance in the upper 400 m of 10–15 Sv amplitude and concluded that it played a strong role in producing the 1992 anomalously cool regional upper ocean temperatures that preconditioned the region for a subsequent relatively severe local climate anomaly. In the Banda Sea, there are observed interannual differences in the amplitude of the sea surface temperature (SST) annual cycle of around 2–3°C [*Boely et al*., 1990] and also in the annual cycle of primary productivity in the Banda Sea [*Waworuntu*, 1999]. *Waworuntu* [1999] also shows a

strong signal of the 1997–1998 ENSO event in TOPEX/Poseidon sea surface height in the central Banda Sea. High sea level occurs at the same time as maximum Makassar Strait through flow in boreal winter 1996–1997 [*Gordon et al*., 1999], while low sea level corresponds to the period of minimal Makassar through flow.

We thus hypothesize that differences in phase of transport at the entrance and exit straits may play an important role in creating the observed interannual SST and sea surface height differences in the Banda Sea and may be significant at other timescales as well. The existence of significant phase differences across the Banda Sea needs to be verified with simultaneous direct measurement of both surface and subsurface flow through both inflow and outflow straits. The unknown contribution of flow through the eastern route from the Pacific to the Banda Sea also needs to be conclusively documented. At this time, however, the recent measurements suggest that the passages gating flow from the Pacific and those gating flow into the Indian Ocean respond to different aspects of the complex blend of Pacific, Indian, and local forcing that characterizes the region. This complexity demands careful consideration in the design of future Indonesian Throughflow monitoring strategies and suggests new avenues for research into the nature and impact of regional mass and heat storage in the interior Indonesian seas.

Acknowledgments. We gratefully acknowledge the commanders and crew of the R/V *Baruna Jaya I* and R/V *Baruna Jaya IV* for their capable and enthusiastic support of the project. We also thank our colleagues at BPPT Indonesia for their organizational efforts and warm collegiality. The Ombai Strait deployments and ADCP surveys were facilitated by combining our field program with the Java Australia Dynamics Experiment (JADE) mooring work, and we are grateful to Michele Fieux and Robert Molcard for making this possible. The field support, technical expertise, and scientific insight of Werner Morawitz, Thomas Moore, and Paul Harvey were an important part of the program. Financial support was provided by the National Science Foundation (OCE-9819511, OCE-9818670, OCE-9505595, OCE-9415897, and OCE-9529641) and the Office of Naval Research (N00014-94-1-0617). Finally, we thank John Toole, whose comments in his capacity as Editor greatly improved the manuscript.

References

Arief, D., A study on low frequency variability in current and sea-level in the Lombok Strait and adjacent region, Ph.D. dissertation, La. State Univ. at Baton Rouge, 1992.

Arief, D., and S. P. Murray, Low-frequency fluctuations in the Indonesian Throughflow through Lombok Strait, *J. Geophys. Res*., *101*, 12,455–12,464, 1996.

Boely, T., et al., Seasonal and interannual variations of the sea surface temperatures (SST) in the Banda and Arafura Sea area, *Neth. J. Sea Res*., *25*, 425–429, 1990.

Bray, N., S. L. Hautala, J. Pariwono, and J. C. Chong, Large-scale sea level, thermocline, and wind variations in the Indonesian throughflow region, *J. Geophys. Res*., *101*, 12,239–12,254, 1996.

Bryden, H. L., D. H. Roemmich, and J. A. Church, Ocean heat transport across 24°N in the Pacific, *Deep Sea Res*., *38*, 297–324, 1991.

Candela, J., R. C. Beardsley, and R. Limeburner, Separation of tidal and subtidal currents in ship-mounted acoustic Doppler current profiler observations, *J. Geophys. Res*., *97*, 769–788, 1992.

Chong, J. C., J. Sprintall, S. Hautala, W. L. M. Morawitz, N. A. Bray, and W. Pandoe, Shallow throughflow variability in the outflow straits of Indonesia, *Geophys. Res. Lett*., *27*, 125–128, 2000.

Clarke, A. J., and X. Liu, Observations and dynamics of semiannual and annual sea levels near the eastern equatorial Indian Ocean boundary, *J. Phys. Ocean*., *23*, 386–399, 1993.

Clarke, A. J., and X. Liu, Interannual sea level in the northern and eastern Indian Ocean, *J. Phys. Ocean*., *24*, 1224–1235, 1994.

Egbert, G., A. Bennett, and M. Foreman, TOPEX/Poseidon tides estimated using a global inverse model, *J. Geophys. Res*., *99*, 24,821–24,852, 1994.

Ffield, A., and A. L. Gordon, Vertical mixing in the Indonesian thermocline, *J. Phys. Ocean*., *22*, 184–195, 1992.

Ganachaud, A., C. Wunsch, J. Marotzke, and J. Toole, Meridional overturning and large-scale circulation of the Indian Ocean, *J. Geophys. Res*., *105*, 26,117–26,134, 2000.

Godfrey, J. S., The effect of the Indonesian Throughflow on ocean circulation and heat exchange with the atmosphere: A review, *J. Geophys. Res*., *101*, 12,217–12,237, 1996.

Gordon, A. L., R. D. Susanto, and A. L. Ffield, Throughflow within Makassar Strait, *J. Geophys. Res. Lett*., *26*, 3325–3328, 1999.

Hatayama, T., T. Awaji, and K. Akitomo, Tidal currents in the Indonesian seas and their effect on transport and mixing, *J. Geophys. Res*., *101*, 12,353–12,373, 1996.

Hautala, S. L., J. L. Reid, and N. Bray, The distribution and mixing of Pacific water masses in the Indonesian seas, *J. Geophys. Res*., *101*, 12,375–12,389, 1996.

Joyce, T. M., On in situ "calibration" of shipboard ADCPs, *J. Atmos. Oceanic Technol*., *6*, 169–172, 1989.

Kashino, Y., M. Aoyama, T. Kawano, N. Hendiarti, Syaefudin, Y. Anantasena, K. Muneyama, and H. Watanabe, The water masses between Mindanao and New Guinea, *J. Geophys. Res*., *101*, 12,391–12,400, 1996.

Labrecque, A. J., R. E. Thomson, M. W. Stacey, and J. R. Buckley, Residual currents in Juan de Fuca Strait, *Atmos. Ocean*, *32*, 375–394, 1994.

MacDonald, A. M., The global ocean circulation: A hydrographic estimate and regional analysis, *Prog. Oceanogr*., *41*, 281–382, 1998.

Meyers, G., Variation of Indonesian throughflow and the El Niño–Southern Oscillation, *J. Geophys. Res*., *101*, 12,255–12,263, 1996.

Meyers, G., R. J. Bailey, and A. P. Worby, Geostrophic transport of Indonesian Throughflow, *Deep Sea Res*., *Part I*, *42*, 1163–1174, 1995.

Michida, Y., and H. Yoritaka, Surface currents in the area of the Indo-Pacific throughflow and the tropical Indian Ocean observed with surface drifters, *J. Geophys. Res*., *101*, 12,475–12,482, 1996.

Molcard, R., et al., Low frequency variability of the currents in Indonesian channels (Savu-Roti and Roti-Ashmore reef), *Deep Sea Res*., *Part I*, *41*, 1643–1661, 1994.

Molcard, R., M. Fieux, and A. G. Ilahude, The Indo-Pacific throughflow in the Timor Passage, *J. Geophys. Res*., *101*, 12,411–12,420, 1996.

Molcard, R. M., et al., The throughflow within Ombai Strait, *Deep Sea Res*., *Part I*, *48*, 1237–1253, 2001.

Münchow, A., R. W. Garvine, and T. F. Pfeiffer, Subtidal currents from a shipboard acoustic Doppler current profiler in tidally dominated waters, *Cont. Shelf Res*., *12*, 499–515, 1992.

Münchow, A., et al., Performance and calibration of an acoustic Doppler current profiler towed below the surface, *J. Atmos. Oceanic Technol*., *12*, 435–444, 1995.

Murray, S. P., and D. Arief, Throughflow into the Indian Ocean through the Lombok Strait, January 1985–January 1986, *Nature*, *333*, 444–447, 1988.

Murray, S. P., et al., Characteristics of circulation in an Indonesian archipelago strait from hydrography, current measurements and modeling results, in *The Physical Oceanography of Sea Straits*, edited by L. J. Pratt, pp. 3–23, Kluwer Acad., Norwell, Mass., 1990.

Pandoe, W. W., Flow pattern in the Ombai Strait, Indonesia, and its relationship with the Indonesian Throughflow, M.Sc. thesis, 87 pp., Tex. A&M Univ., College Station, 2000.

Potemra, J. T., R. Lukas, and G. T. Mitchum, Large-scale estimation of transport from the Pacific to the Indian Ocean, *J. Geophys. Res*., *102*, 27,795–27,812, 1997.

Pratt, L. J., and P. A. Lundberg, Hydraulics of rotating strait and sill flow, *Annu. Rev. Fluid Mech*., *23*, 81–106, 1991.

Qiu, B., Intraseasonal variability in the Indo-Pacific throughflow and the regions surrounding the Indonesian seas, *J. Phys. Ocean*., *29*, 1599–1618, 1999.

Quadfasel, D., and G. R. Cresswell, A note on the seasonal variability of the South Java Current, *J. Geophys. Res*., *97*, 3685–3688, 1992.

Rochford, D. J., Distribution of Banda Intermediate Water in the Indian Ocean, *Aust. J. Mar. Fish. Res*., *17*, 61–76, 1966.

Semtner, A. J., and R. M. Chervin, Ocean general circulation from a global eddy-resolving model, *J. Geophys. Res*., *97*, 5493–5550, 1992.

Sprintall, J., et al., Regional climate variability and ocean heat trans-

port in the southwest Pacific Ocean, *J. Geophys. Res*., *100*, 15,865–15,871, 1995.

Sprintall, J., J. Chong, F. Syamsudin, W. Morawitz, S. Hautala, N. Bray, and S. Wijffels, Dynamics of the South Java Current in the Indo-Australia Basin, *Geophys. Res. Lett*., *26*, 2493–2496, 1999.

Sprintall, J., A. Gordon, R. Murtugudde, and R. D. Susanto, A semiannual Indian Ocean Kelvin wave observed in the Indonesian seas in May 1997, *J. Geophys. Res*., *105*, 17,217–17,230, 2000.

Toulany, B., and C. Garrett, Geostrophic control of fluctuating barotropic flow through straits, *J. Phys. Oceanogr*., *14*, 649–655, 1984.

Van Bennekom, A. J., Deep-water transit times in the eastern Indonesian basins, calculated from dissolved silica in deep and interstitial waters, *Neth. J. Sea Res*., *22*, 341–354, 1988.

Van Riehl, P. M., Introductory remarks and oxygen content, in *The Snellius Expedition*, vol. II, *Oceanographic Results*, *Part V: The Bottom Water*, 77 pp., E. J. Brill, Cologne, Germany, 1943.

Waworuntu, J., Water mass transformations and throughflow variability in the Indonesian seas, Ph.D. dissertation, 97 pp., Univ. of Miami, Coral Gables, Fla., 1999.

Wearn, R. B., Jr., and N. G. Larson, Measurements of the sensitivities and drift of Digiquartz pressure sensors, *Deep Sea Res*., *29*, 111–134, 1982.

Wijffels, S., E. Firing, and H. Bryden, Direct observations of the Ekman balance at 10°N in the Pacific, *J. Phys. Oceanogr*., *24*, 1666–1679, 1994.

Wyrtki, K., Scientific results of marine investigations of the South China Sea and the Gulf of Thailand 1959–1961. NAGA report, vol. 2, 195 pp., Scripps Inst. of Oceanogr., La Jolla, Calif., 1961.

Wyrtki, K., Indonesian Throughflow and the associated pressure gradient, *J. Geophys. Res*., *92*, 12,941–12,946, 1987.

Yu, L., and M. M. Rienecker, Mechanisms for the Indian Ocean warming during the 1997–98 El Niño, *Geophys. Res. Lett*., *26*, 735–738, 1999.

N. Bray, CSIRO Marine Research, GPO Box 1538, Hobart, Tasmania 7001, Australia. (nan.bray@marine.csiro.au)

J. C. Chong and J. Sprintall, Physical Oceanography Research Division 0230, Scripps Institution of Oceanography, La Jolla, CA 92093, USA. (jcchong@aya.yale.edu; jsprintall@ucsd.edu)

S. L. Hautala and J. T. Potemra, School of Oceanography, University of Washington, Box 355351, Seattle, WA 98195, USA. (hautala@u.washington.edu; jimp@ocean.washington.edu)

A. G. Ilahude, Indonesian Institute of Sciences (LIPI), Jln. Pasir Putih I, Ancol Timur, P.O. Box 4801, JKTF Jakarta 11001, Indonesia. (p3o_lipi@jakarta.wasantara.net.id)

W. Pandoe, Department of Oceanography, Texas A&M University, College Station, TX 77843, USA. (wpandoe@ocean.tamu.edu)

(Received July 31, 2000; revised April 10, 2001;
accepted May 21, 2001.)